

# Mathematical Innovation of Zonal Air Supply Design for Enhancing Thermal Comfort in Hot, Humid Climates

Zuhair Jastaneyah<sup>1,2</sup>, Haslinda Mohamed Kamar<sup>2</sup>, Ahmad Hashmi<sup>3</sup>, F. A. Ghaleb<sup>2</sup> and Hakim AL Garalleh<sup>4</sup>

<sup>1</sup>Department of Mechanical Engineering, College of Engineering, University of Business and Technology, Jeddah 21361, Saudi Arabia

<sup>2</sup>Faculty of Mechanical Engineering, University Teknologi Malaysia, Kuala Lumpur 81310, Malaysia

<sup>3</sup>Department of Architectural Engineering, College of Engineering, University of Business and Technology, Jeddah 21361, Saudi Arabia

<sup>4</sup>Department of Mathematical Science, College of Engineering, University of Business and Technology, Jeddah 21361, Saudi Arabia

Received: 24 Dec. 2024, Revised: 3 Feb. 2025, Accepted: 13 Feb. 2025

Published online: 1 May 2025

**Abstract:** Classrooms in hot and humid regions often depend on air conditioning systems with mixing ventilation for cooling. However, this method frequently fails to achieve adequate thermal comfort due to elevated temperatures and inefficient air distribution. This study introduces an innovative zonal air supply demonstrated that adopting a 4-zonal air supply system with stratum ventilation-featuring inlets at 1 meter and outlets at 0.2 meters-reduced the PMV and PPD by design to enhance classroom thermal comfort in Jeddah, Saudi Arabia. Computational Fluid Dynamics (CFD) simulations were utilized to show the distributions of air temperature, velocity, and relative humidity, identifying the optimal zonal air supply configuration for maximizing thermal comfort. Parametric analysis were conducted to optimize the Predicted Mean Vote (PMV) and Percentage of People Dissatisfied (PPD) indices. The results reveal that, under the current ventilation setup, the indices values at three heights within the classroom Surpass the upper thresholds established by ASHRAE Standard-55, highlighting a significant need for improved thermal comfort. The parametric flow analysis indices by 69-98% and 64-74%, respectively. These results confirm that this approach substantially enhances thermal comfort in the classroom environment.

**Keywords:** Classroom; Stratum ventilation, Mixing ventilation, Displacement ventilation, Computational fluid dynamics simulation, Thermal comfort, Hot, Humid climate; Predicted Mean Vote (PMV); Predicted Percentage of Dissatisfied (PPD); Zonal air supply design.

## 1 Introduction

Thermal comfort has a significant impact on spaces where people remain for long duration's. it greatly impacts their productivity, well-being, and satisfaction with indoor conditions. According to ASHRAE, thermal comfort is defined as a mental state that expresses contentment with the thermal environment" [1]. Ventilation is widely recognized as the most commonly employed method for achieving thermal comfort. Ventilation systems enable the intake of fresh outside air and the expulsion of indoor air, promoting heat exchange and lowering internal temperatures [2,3].

Building ventilation systems are generally classified into three primary types: mechanical, natural, and hybrid [4]. Natural ventilation leverages apertures like windows and

doors or harnesses natural forces like wind to facilitate air movement [5,6]. Mechanical ventilation, on the other hand, depends on equipment like fans and exhaust units to regulate indoor air quality and maintain thermal comfort [7]. Although natural ventilation is often preferred in hot and humid climates for its straightforward nature, it may not be entirely effective due to fluctuations in airflow and other climate-related variables [8].

Maintaining thermal comfort in educational settings is critical for creating a conducive atmosphere that supports effective teaching and learning. Although research has been conducted worldwide on thermal comfort in educational settings, there is a significant shortage of in-depth research concentrating on classrooms in Jeddah, Saudi Arabia [9,10,11]. In Jeddah, air conditioning systems with mixing ventilation are predominantly used

\* Corresponding author e-mail: [h.algaralleh@ubt.edu.sa](mailto:h.algaralleh@ubt.edu.sa)

to regulate thermal comfort in classrooms [12]. However, achieving satisfactory thermal comfort is a challenge due to the city's climate, where typical temperatures vary between 27 °C and 32 °C and humidity levels vary between 55% and 70% [9]. Although mixing ventilation helps in air circulation, it does not always provide uniform air distribution or stable temperature regulation. Therefore, alternative strategies should be explored to enhance the efficiency of conventional mixing ventilation systems in classrooms across Jeddah.

Many indices have been found to determine thermal comfort in indoor environments [13]. Nevertheless, several of these indices present certain limitations, as they are tailored for specific climatic conditions. The Predicted Mean Vote (PMV) and Predicted Percentage Dissatisfied (PPD) indices are now widely recognized as the standard methods for evaluating thermal comfort across a variety of indoor settings [14, 15, 16, 17]. The PMV estimates the average thermal sensation experienced by individuals on a seven-point scale [1, 18]. In contrast, the PPD predicts the percentage of people likely to experience discomfort from being either too hot or too cold [19].

Various methodologies are used to evaluate ventilation system performance, such as empirical, analytical, zonal, and multi-zone models, as well as small-scale and full-scale experimental approaches and Computational Fluid Dynamics (CFD) simulations [3]. CFD, in particular, has become a preferred approach due to its precision in predicting ventilation parameters, benefiting greatly from advancements in computational technology [3, 20, 21]. Numerous studies have successfully combined CFD with experimental methods to assess indoor thermal comfort [15, 17, 22, 23, 24, 25, 26, 27, 28, 29, 30, 31, 32, 33]. This paper details a study on improving thermal comfort within a classroom at the University of Business and Technology (UBT), Jeddah, Saudi Arabia, by integrating field measurements, student feedback, and CFD modeling. The main objective is to identify the most effective zonal air supply strategy to enhance classroom thermal comfort. PMV and PPD indices were utilized for the evaluation, following the standard procedures set by the ISO.

## 2 Methodology

### 2.1 Climate

Jeddah, a major urban hub in western Saudi Arabia, is situated along the Red Sea at a latitude of 21° 54' north and a longitude of 39° 7' east [29]. The city experiences a hot and humid tropical climate, typical of this region [29, 30, 31]. High temperatures and humidity levels are prevalent, with average air temperatures varying between 27 °C and 32 °C and relative humidity levels fluctuating from 55% to 70% [4]. The hottest temperatures are

recorded in July, peaking at 48.5 °C, while the lowest temperature, 23.8 °C, is observed in June [32, 33].

### 2.2 Field Measurements

A field study was carried out in a classroom at the University of Business and Technology in Jeddah, Saudi Arabia. Fig. 1(a) provides an external view of the university, while Fig. 1(b) depicts the specific classroom selected for the study. Located on the second floor, as outlined in the floor plan in Fig. 2, the classroom dimensions are 9 meters in length, 9.6 meters in width, and 3 meters high. The east wall includes three windows, each 2.4 meters by 1.4 meters, giving a window-to-wall ratio (WWR) of 40%, and each window has an area of 3.6 square meters. On the west side are two doors—one measuring 2.1 meters in height by 1.6 meters in width and the other 2.1 meters by 0.9 meters. The classroom has a split duct air conditioning system with seven supply diffusers and eight extract grilles on the ceiling, each measuring 0.6 by 0.6 meters. Figure 3 shows the room's layout of inlets, outlets, doors, and windows.

The study measured thermal comfort factors such as air temperature, air velocity, relative humidity, and globe temperature. Consistent with other research on classroom environments [34, 35, 36], measurements were taken at the room's center at heights of 0.1 m, 0.6 m, and 1.1 m above the floor, following ASHRAE Standard 55 [1, 37], as illustrated in Fig. 4. The mean radiant temperature was then calculated using the formula in the ASHRAE Handbook [38], as detailed in Equation (1).

$$T_{mrt} = [(T_g + 73)^4 + \frac{1.1 * 10^{0.8} * V_a^{0.6}}{\epsilon * D^{0.4}} (T_g - T_a)]^{1/4} - 273, \quad (1)$$

where  $T_a$  is the air temperature (°C),  $T_g$  is the globe temperature (°C),  $\epsilon$  is the emissivity of the globe, and  $D$  is the diameter of the globe. The value of  $\epsilon$  is 0.95 for the black globe, and  $D$  is 0.04 m [39].

Data collection took place in July 2024, recognized as the hottest month of the year [37], aligning with similar studies conducted during the summer semester [40, 41]. Measurements were obtained every ten minutes from 8:30 AM to 5:30 PM on Sundays, Tuesdays, and Thursdays, coinciding with lecture times. To ensure accuracy, specialized instruments, each certified for calibration, were employed for the measurements. An uncertainty analysis was conducted to determine the percentage of uncertainty, as illustrated in Figure 5. Details about the instruments used are illustrated in Table 1. Meanwhile, Table 2 presents the air temperature, relative humidity, and airflow velocity uncertainties derived from the field data.



**Fig. 1:** (a) The university building and (b) the case study classroom.

**Table 1:** CFD model of the case study classroom.

Climate Parameters	Measuring Tool	Accuracy
Air velocity	Testo 405i, Thermal Anemometer	(0.1 m/s + 5% of mv) (0 to 2 m/s) (0.3 m/s + 5% of mv) (2 to 15 m/s)
Air temperature	Hot Wire Anemometer (HHF-SD1)	± (0.4% + 0.5 °C)
Relative humidity	HOBO Relative Humidity Data Logger (H14-001)	3.0% RH (10 to 35% RH) (at 25 °C) 2.0% RH (35 to 65% RH) (at 25 °C) 3.0% RH (65 to 90% RH) (at 25 °C) 5.0% RH (≥ 10% RH or ≤ 90% RH)
Globe temperature	HOBO Relative Humidity Data Logger (H14-001)	2 °C (15 to 40 °C)
wall temperature	HOBO Data Logger (UX120)	2 °C (15 to 40 °C)

**Table 2:** Uncertainty of parameters.

	Parameters											
	Globe temperature (°C)			Air temperature (°C)			Relative humidity (%)			Relative humidity (m/s)		
Height (m)	0.1	0.6	1.1	0.1	0.6	1.1	0.1	0.6	1.1	0.1	0.6	1.1
Minimum (y)	25.8	25.9	25.7	24.2	24.3	24	49	48	49	0.01	0.01	0.03
Maximum (X)	27	27.1	26.9	25.4	25.6	25.1	50	49	50	0.02	0.02	0.04
Mean ( $\bar{X}$ )	26.4	25.5	26.3	24.7	24.8	24.5	49	48	50	0.01	0.01	0.04
Standard deviation ( $\sigma$ )	0.15	0.11	0.12	0.13	0.11	0.1	0.2	0.2	0.27	0.004	0.005	0.002
Standard uncertainty ( $X \pm \sigma$ )	26.4±0.15	26.5±0.11	26.3±0.12	24.7±0.13	24.8±0.11	24.3±0.1	49±0.2	48±0.22	50±0.26	0.01±0.0004	0.01±0.0005	0.04±0.0009
Percentage of uncertainty	5%	4%	4.5%	5%	4%	4%	4%	4.5%	5%	4%	5%	2.3%

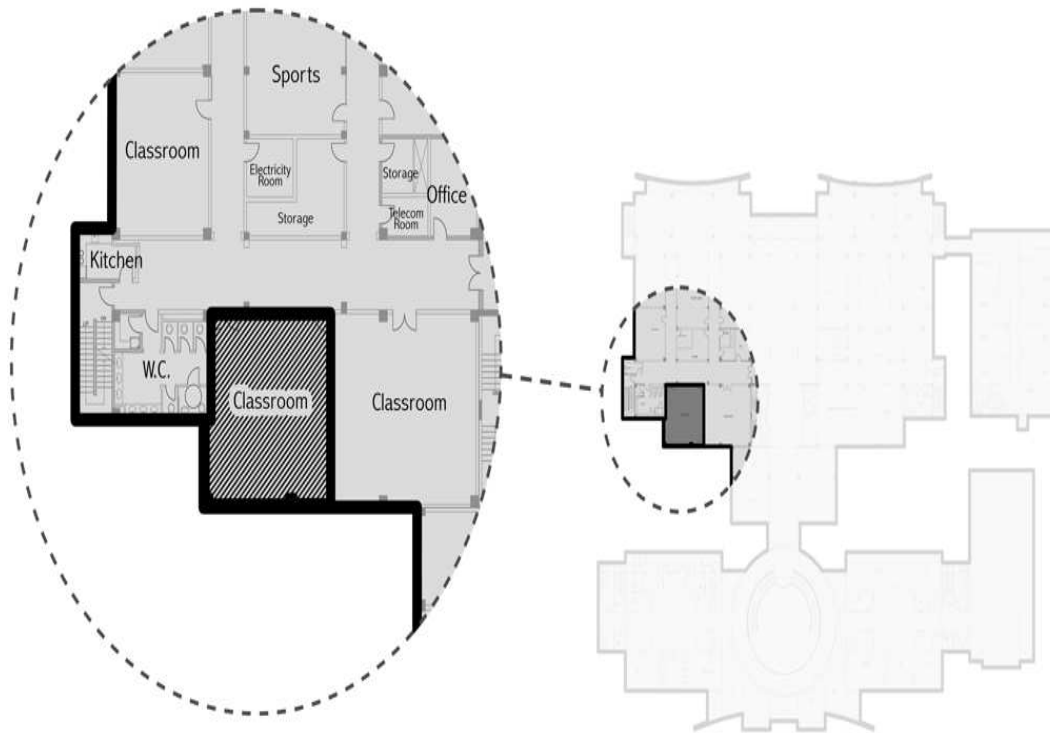


Fig. 2: Floor plan of the second floor showing the classroom's location.

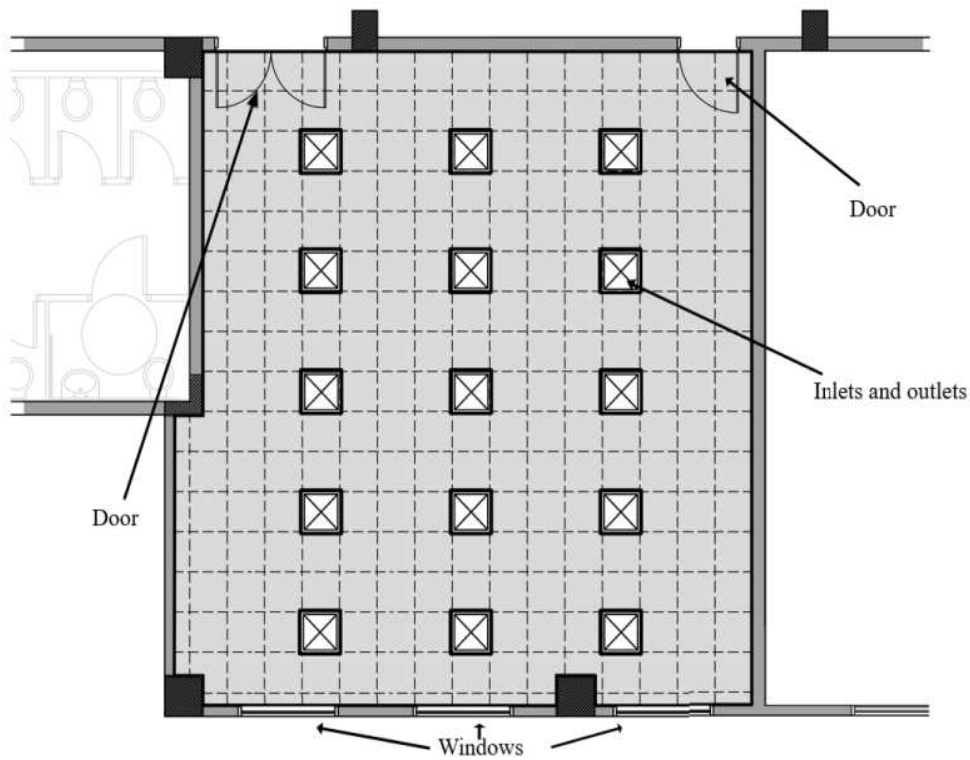


Fig. 3: Location of inlets, outlets, doors and windows.



Fig. 4: Position and height of the measuring instrument.

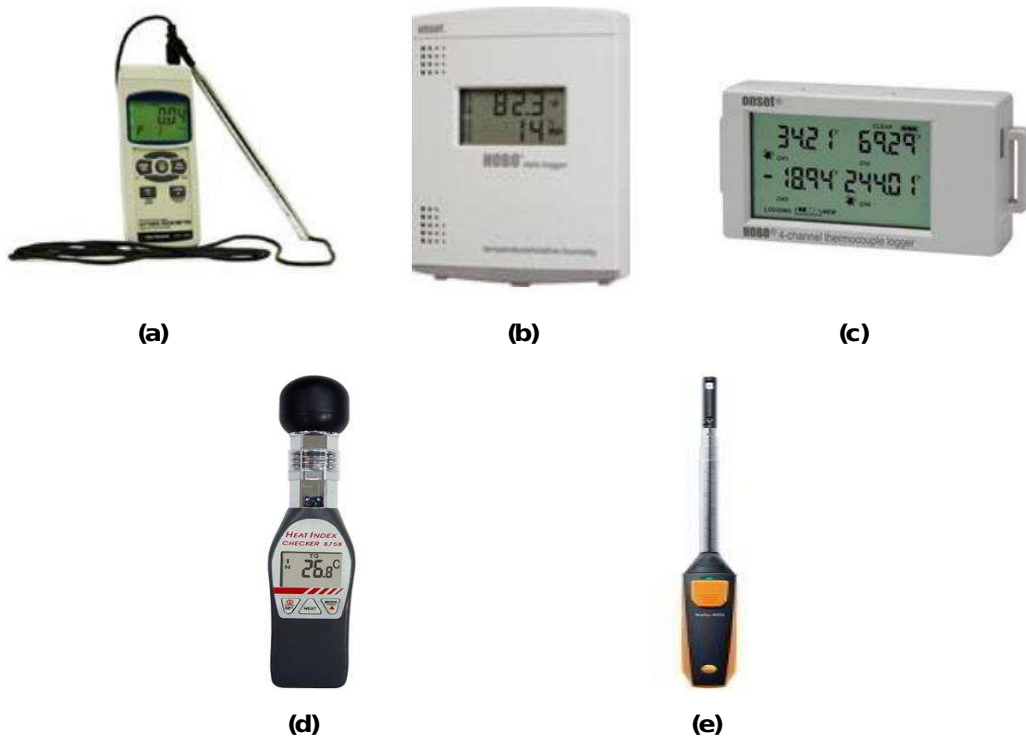


Fig. 5: Instruments used for field measurements.

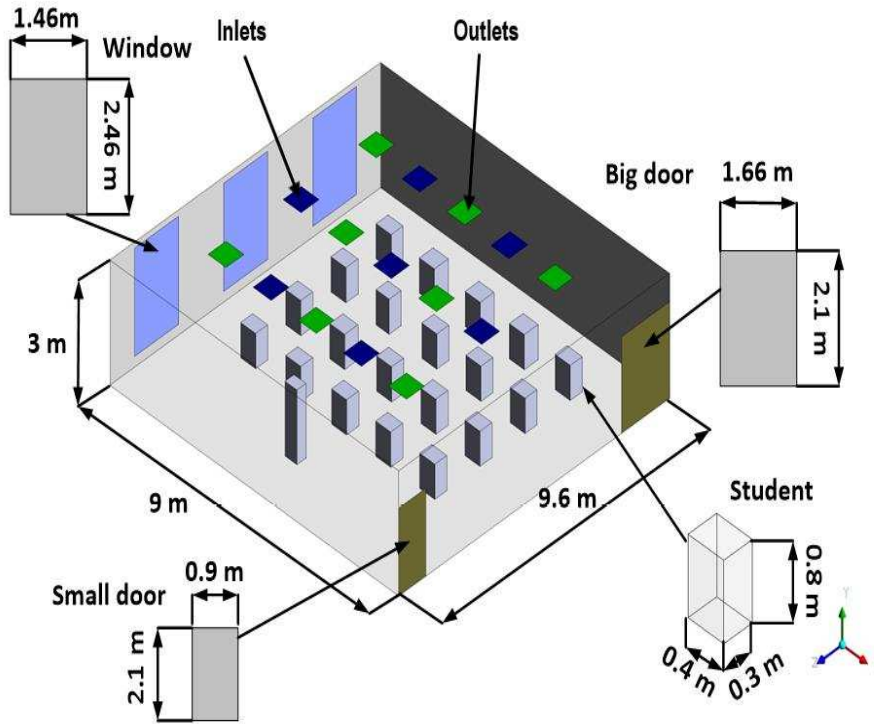


Fig. 6: Classroom's model.

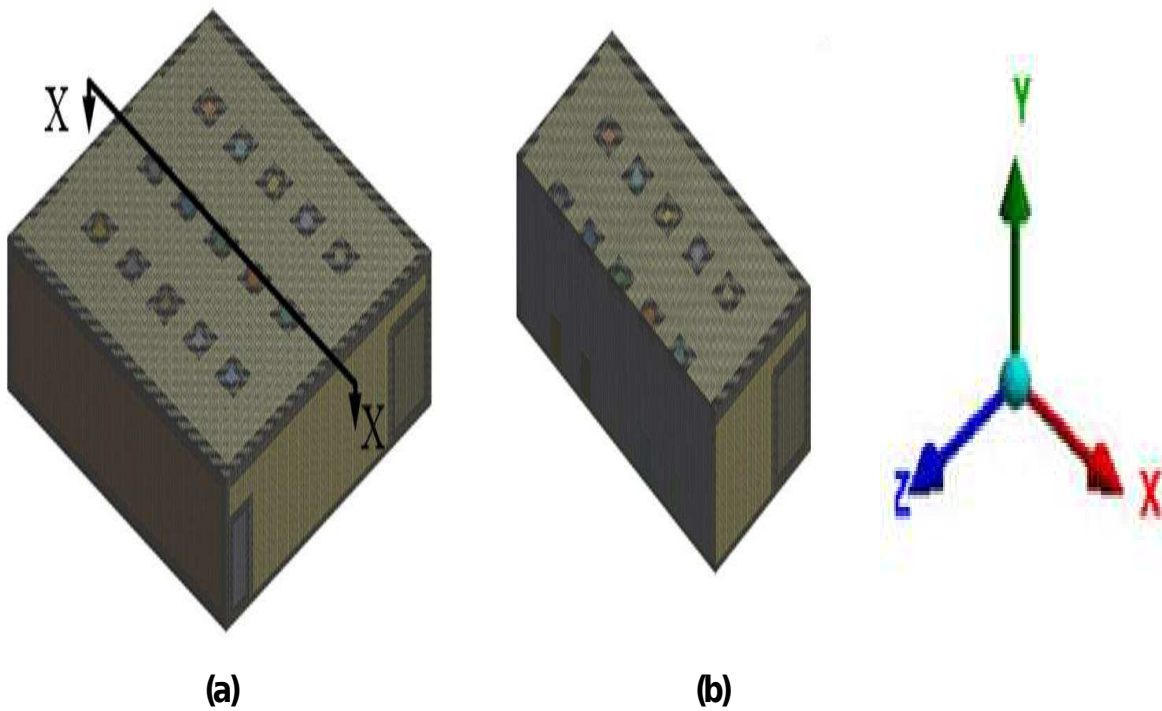


Fig. 7: (a) Computational domain meshing, (b) Cross-sectional view (x-x) of the domain.

### 2.3 Calculations of Indices

The Predicted Mean Vote (PMV) and Percent of People Dissatisfied (PPD) indices were applied using the CBE thermal comfort tool to evaluate thermal comfort in the classroom [42]. The PMV index quantitatively represents the thermal interactions between the body and the environment [28]. It predicts the average thermal sensation of a large group of individuals, as defined by the ASHRAE thermal sensation scale. ASHRAE Standard 55 [1, 20] recommends maintaining PMV values within the range of -0.5 to +0.5 for indoor settings. In contrast, the PPD index estimates the percentage of occupants likely to experience discomfort under the given thermal conditions. The PMV value is calculated using Equation (2) [28].

$$PMV = [0.303 e^{-0.036M} + 0.028]L, \quad (2)$$

where

$$L = M - W - (3.96 * 10^{-8} f_{cl} [(T_{cl} + 273) * 4] + f_{cl} h_c (T_{cl} - T) + [5733 - 6.99(M - W) - P_v] + 0.42(M - W - 58.15) + 1.7 * 10^{-5} M (5867 - P_v) + 0.0014M(34 - T)), \quad (3)$$

where  $W$  is the active work ( $W/m^2$ ),  $P_v$  is the water vapor partial pressure obtained from the ASHRAE standard-55,  $T(^{\circ}C)$  is the local air, and  $f_{cl}$  is the garment insulation factor given by

$$f_{cl} = \begin{cases} 1.05 + 0.645 \times I_{cl} & \text{for } I_{cl} \geq 0.078 \\ 1 + 1.291 \times I_{cl} & \text{for } I_{cl} < 0.078 \end{cases} \quad (4)$$

where  $I_{cl}$  refers to the resistance to sensible heat transfer offered by the clothing ( $mK/W$ ),  $T_{cl}$  ( $^{\circ}C$ ) is the clothing temperature given by

$$T_{cl} = 35.7 - 0.028(M - W) - I_{cl}. \quad (5)$$

The heat transfer coefficient  $h_c$  ( $W/m^2$ ) is between the air and the cloth given by

$$h_c = \begin{cases} 2.38(T_{cl} - T) & \text{if } 2.38(T_{cl} - T) > 12.1u^{0.5} \\ 12.1u^{0.5} & \text{if } 2.38(T_{cl} - T) < 12.1u^{0.5} \end{cases} \quad (6)$$

where  $u$  is the local velocity ( $m/s$ ). The predicted percentage dissatisfied (PPD) is a function of PMV and is calculated by using the equation below

$$PPD = 100 - e^{(-0.03353 \times (PMV)^4 + 0.2179 \times (PMV)^4)}. \quad (7)$$

### 2.4 Computation Fluid Dynamics Analysis

This study employed Computational Fluid Dynamics (CFD) simulations to model the distribution of air

temperature, relative humidity, and air velocity at three heights within the classroom. The simulations were conducted for both the existing ventilation setup and hypothetical scenarios involving the implementation of zonal air supply systems. The findings were used to compute thermal comfort indices, which were then validated against the field measurement data. Using ANSYS FLUENT software, a computational domain that accurately represented the classroom geometry was developed for analysis. Following this, a parametric study was conducted to assess the effectiveness of two different zonal air supply configurations in enhancing classroom thermal comfort. The CFD process comprised multiple stages, including developing a simplified classroom model, generating the mesh, defining boundary conditions, and configuring solution methodologies.

The analysis followed a systematic approach, beginning with creating a simplified geometric model of the classroom, setting up boundary conditions, and selecting appropriate solution strategies. The RNG  $k - \zeta$  model was applied due to its reliability and accuracy in simulating indoor environments [41, 43, 44]. Additionally, a species transport model was introduced to analyze the air-water vapor mixture, which allowed for predicting relative humidity levels within the classroom [45]. The corresponding species transport equation is provided below [26].

#### 2.4.1 Geometry

A simplified model of the classroom was created in ANSYS software using its real dimensions, as shown in Fig. 6. This model represents the baseline scenario for CFD analysis under the existing ventilation conditions. Certain elements like furniture and lighting fixtures were omitted to streamline the geometry. However, essential features were retained, including 21 occupants (20 students and one instructor) represented by square shapes, two doors on the west wall, and three windows on the east wall. The occupants were modeled with average dimensions of 1.6 meters in height, 0.40 meters in width, and 0.30 meters in thickness, ASHRAE Standard 55 [1]. Each occupant was depicted in a seated position at a height of 0.8 meters [40].

$$\frac{d}{dt}(\rho c) + \frac{d}{dx}(\rho uc) + \frac{d}{dy}(\rho vc) + \frac{d}{dz}(\rho wc) = D_c \left( \frac{d^2 c}{dx^2} + \frac{d^2 c}{dy^2} + \frac{d^2 c}{dz^2} \right) + S_c, \quad (8)$$

where  $c$  is the mixture concentration,  $\rho$  is the mixture's density,  $S_c$  is the generation rate of the mixture and  $D_c$  is the diffusion coefficient.

The analyses were performed until satisfactory convergence of all residuals was attained. For validation purposes, it is advisable to use lower residual values to ensure a fully converged solution [46].

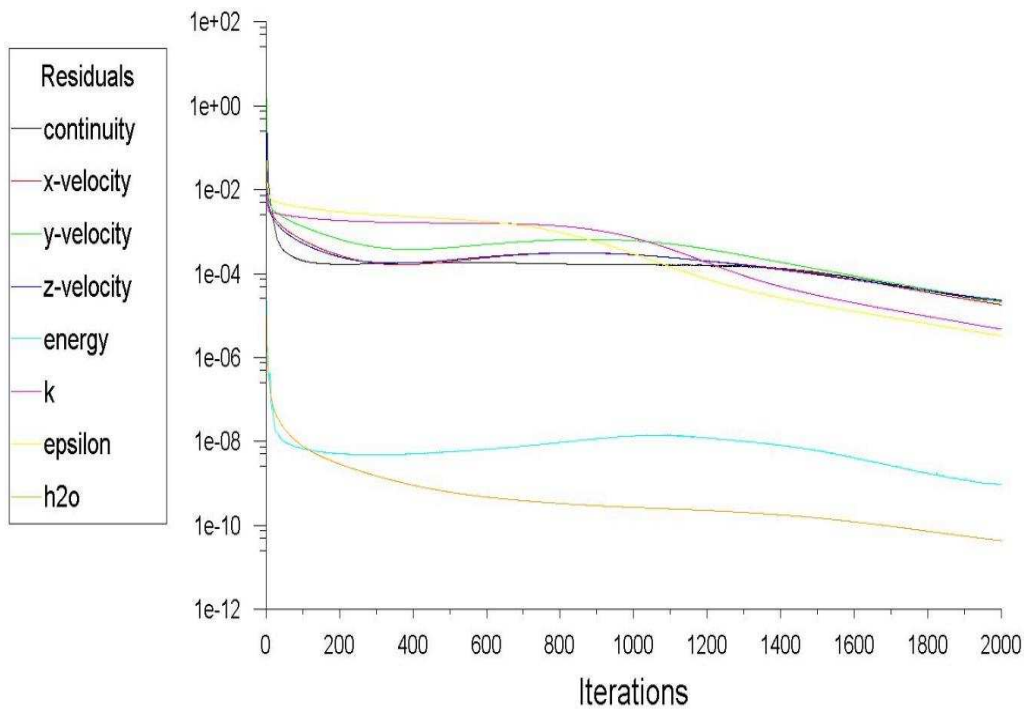


**Fig. 8:** Residuals of the CFD analysis.

**Table 3:** Baseline boundary conditions.

Section	Boundary condition	parameters
Inlet	Inlet air	$V_a = 0.571$ m/s $T_a = 20$ °C Species mass fraction: 0.0076
Outlet	Outlet air	Pressure $e = 0$ Pa (guage)
Roof wall		$T = 27$ °C
North wall		$T = 24$ °C
East wall		$T = 30$ °C
Wall	South wall	Temperature $T = 24$ °C
	West wall	$T = 24$ °C
	Floor wall	$T = 20$ °C
	Windows	$T = 32$ °C
	Door	$T = 20$ °C

**Table 4:** Material Properties [1].

Properties	Air	Water vapor	Concrete	Glass	Wood
Density ( $m^3/kg$ )	1.18653	0.0091	2400	2500	700
Thermal conductivity ( $W/m.k$ )	0.0255966	0.0198	0.9	0.8	0.173
Specific heat ( $J/kg.K$ )	1006.1	2014	880	840	2310
Molecular weight ( $kg/kg.mol$ )	28.966	18.01534	—	—	—
Viscosity ( $kg/ms$ )	$1.8205 \times e^{-0.5}$	$1.34 \times e^{-0.5}$	—	—	—

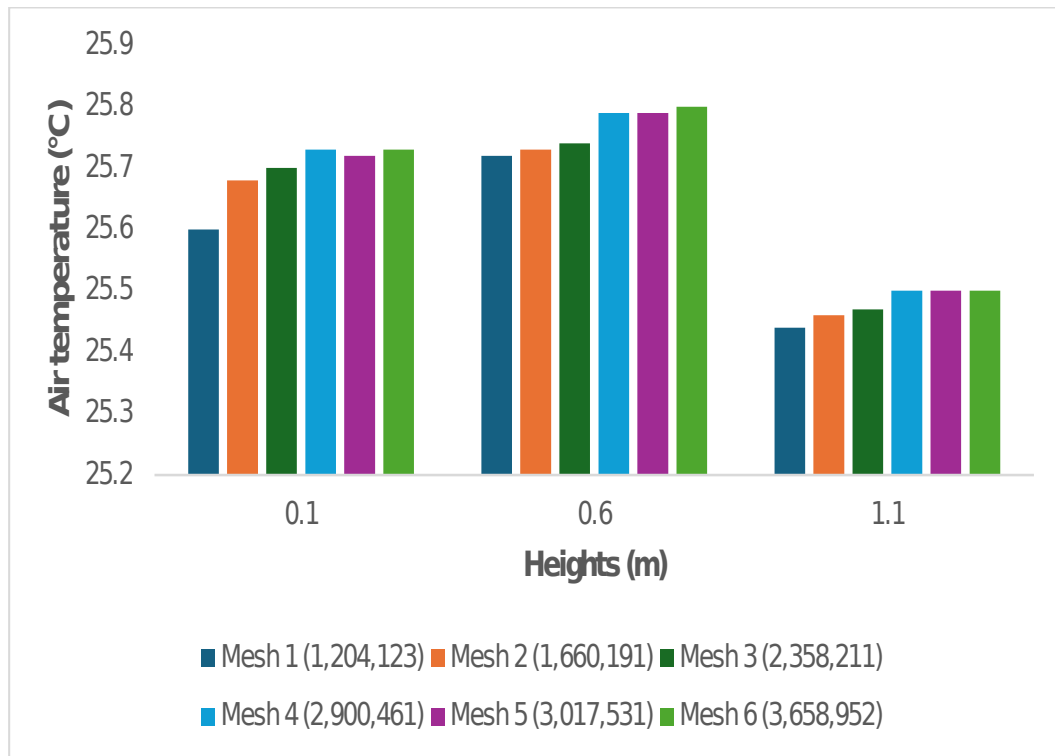


**Fig. 9:** Effect of grid size on air temperature inside the classroom.

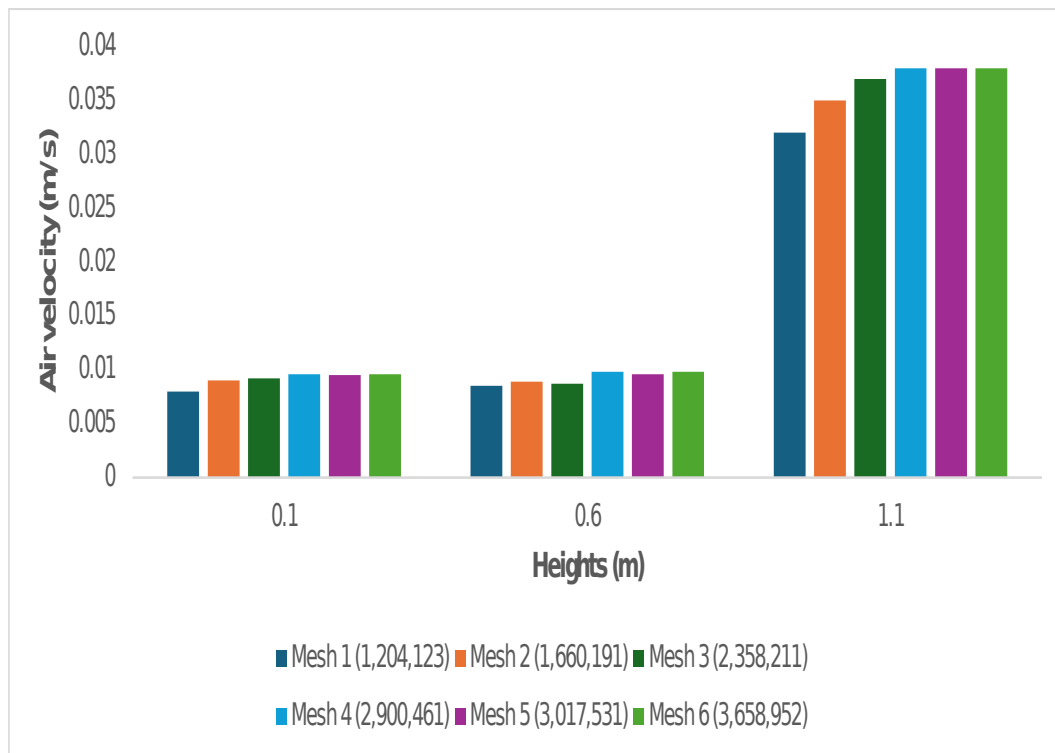


**Fig. 10:** Effect of grid size on air velocity inside the classroom.

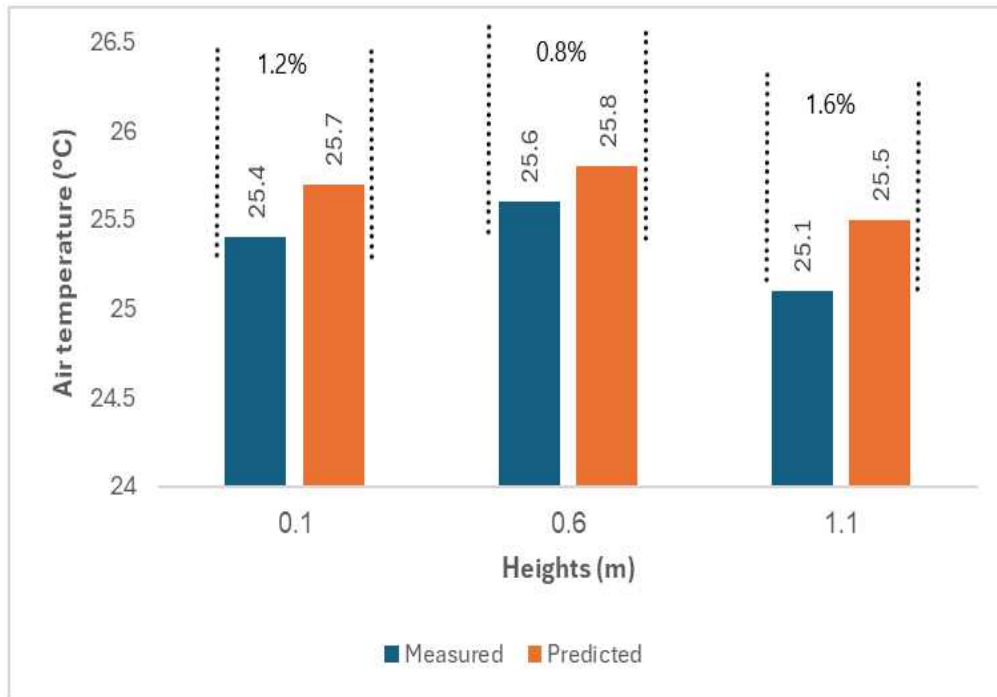


Fig. 11: Predicted and measured air temperature the three heights.

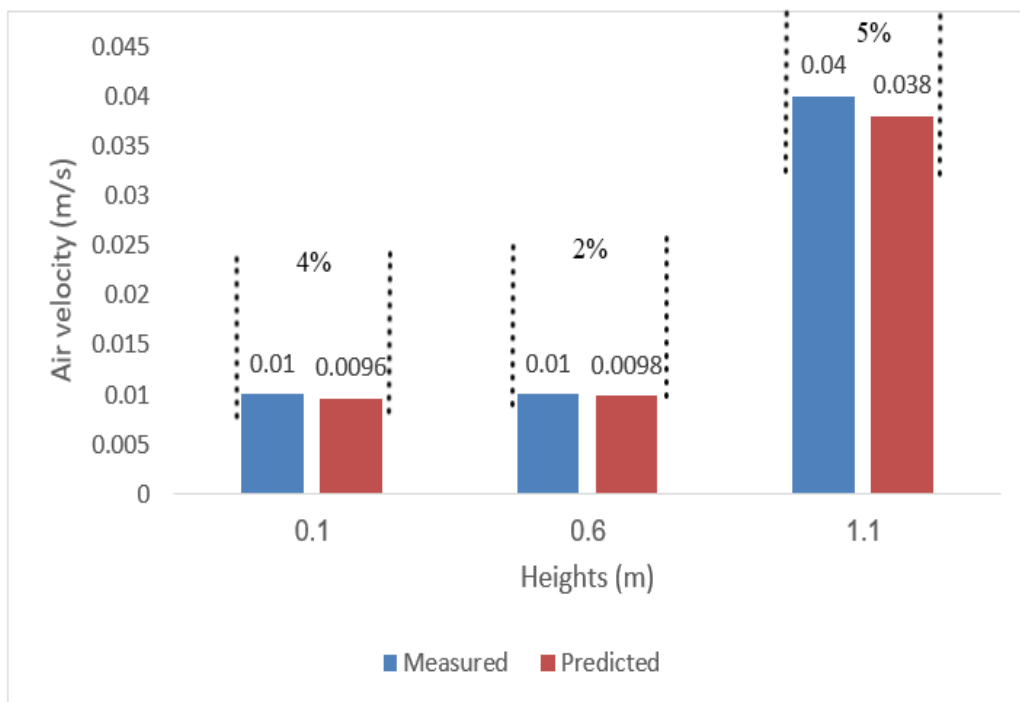


Fig. 12: Predicted and measured air velocity at the three heights.

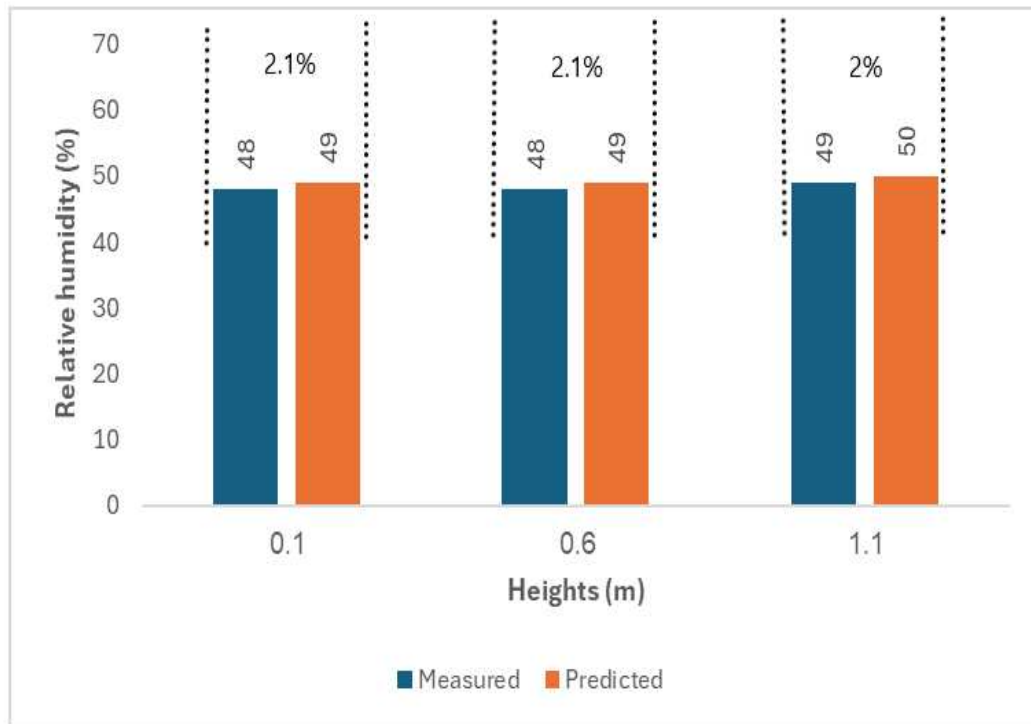


Fig. 13: Predicted and measured relative humidity at the three heights.

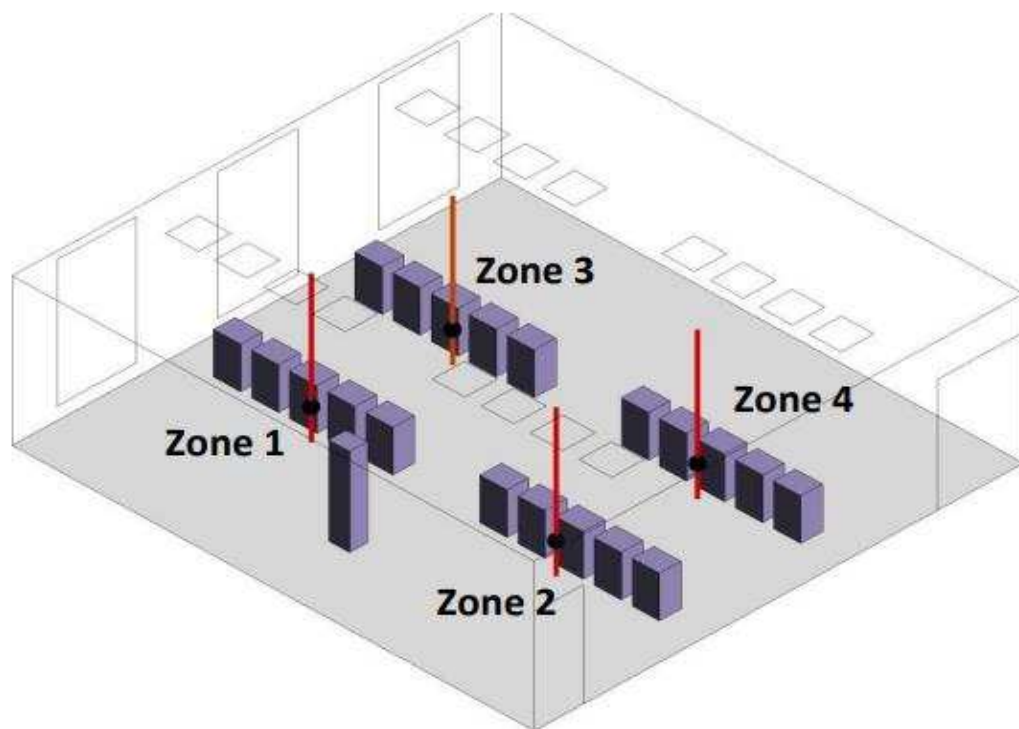


Fig. 14: Four zonal air supply system.

### 2.4.2 Meshing

The classroom interior was meshed using Cut Cell elements, as illustrated in Fig. 7. This technique employs a Cartesian approach with patch-independent volume meshing and advanced size functions. Finer mesh elements were applied near critical areas such as inlets, outlets, doors, and windows to optimize computational efficiency. In contrast, medium-sized elements were utilized in zones adjacent to these features. Coarser mesh elements were assigned to the remaining areas of the computational domain, adopting a meshing strategy that efficiently reduces computational time for CFD flow simulations [15, 16].

### 2.4.3 Boundary Conditions

The boundary conditions for the classroom's computational domain were defined based on parameters obtained from actual field measurements, including airflow velocity, air temperature, relative humidity, and wall temperature. The data collected on July 10, 2024, was selected for the simulation as it recorded the month's highest temperature. In this study, a zero-gauge pressure was set for the outlets. Table 3 summarizes all boundary conditions applied in the CFD model. The properties of air, water vapor, and concrete utilized in the simulations were obtained from the literature [1] and are listed in Table 4. The characteristics of the occupants are provided in Table 5.

### 2.4.4 Solver, Solution Methods and Convergence

A pressure-based solver was selected for the CFD simulations due to its versatility in accommodating various flow regimes, ranging from low-speed incompressible to high-speed compressible flows. This solver provides several advantages, such as reduced memory usage and enhanced flexibility. To reach higher accuracy, a second-order upwind interpolation method was implemented, which is particularly suitable when using tetrahedral meshes or when the flow direction is misaligned with the grid. A SIMPLE algorithm was used to couple velocity and pressure [26, 47], known for its robustness and stability.

The CFD solution was considered converged when the residuals for all governing equations fell below  $10^{-4}$ , while the residual for the energy equation was set at  $10^{-6}$  [21]. This convergence criterion was achieved after 1,840 iterations, as shown in Fig. 8.

### 2.4.5 Grid Independence Test

To ensure the accuracy of the flow simulation results, a grid independence test was conducted on the baseline

CFD model of the classroom to identify the optimal number of elements required to minimize errors [48]. This test involved running simulations on the baseline model using the boundary conditions specified in Section 2.5.3 and the solution setup detailed in Section 2.5.4, consistently applying the RNG  $k - \zeta$  turbulence model throughout. The process began with a coarse mesh of 1,204,123 elements, and airflow velocity and air temperature were monitored at five data collection points within the classroom. The simulation was then repeated with increasingly finer meshes until further refinement no longer produced significant changes in airflow velocity and air temperature across all measured heights. The results of this grid independence test are presented through histogram plots: Figure 9 illustrates the air temperature distribution, while Figure 10 displays the air velocity distribution. These plots confirm that a mesh size of 2,900,461 elements is sufficient to ensure that meshing errors have a negligible influence on the simulation outcomes.

### 2.4.6 Grid Convergence Index

The Grid Convergence Index (GCI) method was employed to evaluate the grid convergence error [49]. According to prior studies, achieving grid convergence typically requires a GCI value of less than 5% [17]. It is crucial to understand that the GCI outcome is affected by factors such as monotonic convergence, oscillatory convergence, and divergence [12]. These convergence conditions depend on the convergence ratio, determined using Equation 9 [50].

$$R = \frac{f_{\text{medium}} - f_{\text{fine}}}{f_{\text{coarse}} - f_{\text{medium}}}, \quad (9)$$

where  $f_{\text{medium}}$ ,  $f_{\text{fine}}$  and  $f_{\text{coarse}}$  are the solutions of the medium, fine, and coarse meshes, respectively, and the convergence conditions are [60]:

$$\begin{cases} \text{Monotonic convergence} & \text{if } 0 < R < 1 \\ \text{Oscillatory convergence} & \text{if } -1 < R < 0 \\ \text{Monotonic divergence} & \text{if } R > 1 \\ \text{Oscillatory divergence} & \text{if } R < -1 \end{cases}$$

Grid convergence error assessment using the GCI method is applicable exclusively under the condition of monotonic convergence. In cases where monotonic convergence is not observed, the grid convergence error is determined using Equation 10 [12, 50].

$$GCI_{\text{fine}} = \frac{F_s \times |\varepsilon|}{r^P - 1}, \quad (10)$$

where  $P$  is the order of convergence,  $\varepsilon$  is the relative difference between the coarse and fine solutions, and  $F_s$  is the safety factor, and  $r$  is the refinement ratio. The relative

difference between the coarse and fine grid solution is given by Equation 11

$$\epsilon = \frac{f_{coarse} - f_{fine}}{f_{fine}} \quad (11)$$

When assessing two grids, a safety factor of 3.0 is generally recommended, whereas a reduced safety factor of 1.25 is suggested when comparing three or more grids [50]. The order of convergence for these comparisons can be calculated using Equation 12

$$P = \frac{\ln \frac{f_{fine} - f_{medium}}{f_{medium} - f_{coarse}}}{\ln(r)} \quad (12)$$

where the refinement ratio  $r$  is calculated using Equation 13 [17]

$$P = \left( \frac{Mesh_{fine}}{Mesh_{coarse}} \right)^{1/3} \quad (13)$$

such that  $r > 1.3$  to separate the discretization error from other sources' errors [51].

In this study, the convergence ratio for both air temperature and airflow velocity was calculated using three different mesh sizes: Mesh 1 (coarse), Mesh 2 (medium), and Mesh 3 (fine), with maximum element counts of 1,204,123, 2,900,461, and 3,658,952, respectively. The calculated convergence ratio ( $R$ ) for air temperature and air velocity were -0.057 and -0.0892, indicating oscillatory convergence conditions. Under these conditions, it is suitable to compute the Grid Convergence Index (GCI) values using equation 10.

The GCI values calculated for air temperature and air velocity for the three mesh sizes are provided in Table 6. The table shows that the GCI values for air temperature and air velocity are 0.016% and 0.039%, respectively, well below the 5% threshold. This indicates that the solution obtained with the finest mesh is effectively grid-independent [21]. Therefore, based on the results from the Grid Independence Test and the Grid Convergence Index analysis, a grid size of 2,900,461 elements was chosen and consistently used throughout the Computational Fluid Dynamics (CFD) simulations. The model's mesh quality was examined using skewness, orthogonal quality, and element quality criteria. The 2,900,461-element model achieved values of 0.13, 0.98, and 0.99, respectively, while maintaining an ideal  $Y^+$  range of 30 to 300 [23,50]. Full mesh specifications are in Table 7.

#### 2.4.7 Validation

Flow simulation using the boundary conditions outlined in Section 2.3.3 and the solution setup described in Section 2.3.4 was carried out to validate the CFD model of the baseline case. The simulation employed the RNG  $k - \zeta$  turbulence model to predict airflow behavior, while

the species transport model was used to simulate moisture distribution within the air. Upon completion of the simulation, air temperature, airflow velocity, and humidity levels were recorded at three different heights inside the classroom. These results were then compared to field measurements collected on July 10, 2021, when the highest temperature of the month was observed. As illustrated in Figs. 11, 12, and 13, the discrepancies between the predicted values obtained for the field measurements for temperature, airflow velocity, and relative humidity were within the ranges of 0.8% to 1.6%, 2% to 5%, and 2% to 2.1%, respectively. Since a deviation of  $\pm 5\%$  is generally deemed acceptable [28, 29], the numerical predictions showed strong alignment with the collected field data, indicating that the CFD model shows sufficient accuracy for the classroom's indoor air conditions.

#### 2.4.8 Innovation of zonal air supply design

A parametric study using CFD was conducted to examine the impact of different 4-4-zonal air supply designs, as shown in Fig 14, on thermal comfort within the classroom. By selecting an appropriate ventilation system and optimizing the positions of inlets and outlets, it is possible to achieve more uniform and controlled airflow conditions, thereby enhancing thermal comfort. This study specifically explored the effects of zonal air supply on mixing, displacement, and stratum ventilation, comparing these to the existing mixing ventilation system in the classroom. Following this, additional parametric studies were performed to analyze how varying the positions of inlets and outlets would affect the chosen ventilation systems. A summary of the cases investigated can be found in Table 8. The boundary conditions for all scenarios remained consistent with those outlined in Tables 3, 4, and 5. Notably, the airflow velocity for the inlets was recalculated for the proposed cases, which featured eight inlets compared to the seven in the baseline scenario.

### 3 Results

#### 3.0.1 Effect of ventilation with zonal air supply

CFD simulations of the 4-zonal air supply assessed mixing, displacement, and stratum ventilation for classroom thermal comfort. Figure 15 shows air velocity distribution, with mixing ventilation ranging from 0 to 0.17 m/s. At 0.1 m and 0.6 m heights, velocities are 0.11-0.14 m/s in the northern and southern areas and 0.05 m/s in occupied zones, with localized higher velocities at 0.6 m. At 1.1 m, velocities reach 0.17 m/s near inlets and 0.02-0.05 m/s in the center. Case 2 with displacement ventilation shows 0-0.12 m/s, higher near inlets at 0.1 m

and 0.6 m, and reducing to 0-0.04 m/s in the center. Velocities at 1.1 m are 0?0.1 m/s in the north/south and 0.02-0.04 m/s in occupied zones. Case 3 with stratum ventilation shows velocities of 0-0.2 m/s, higher near inlets (north) and outlets (south), and 0-0.04 m/s in occupied zones. At 1.1 m, velocities peak at 0.14-0.2 m/s in front of the first row and are 0.0-0.06 m/s in the middle. Each ventilation strategy has unique pros and cons, with mixing ventilation creating dynamic airflow but risking discomfort in occupied zones. With the 4-zonal air supply and mixing ventilation, temperatures range from 22.4°C to 27.2°C, cooler in the north and south (22.4?23.6°C) and warmer in the east (up to 26°C). Displacement ventilation shows temperatures of 22.4?24.8°C, with the coolest areas (22.4?23.2°C) along the edges and warmest on the east side. Case 3, with stratum ventilation, maintains air temperatures between 22°C and 25°C, with the highest values on the eastern edge. At 0.1 m, temperatures range from 22°C to 23.5°C, and at 0.6 m and 1.1 m, they increase slightly in the south and east. Case 3 provides the most uniform temperature distribution, avoiding extremes compared to Case 2, which has the lowest overall temperatures, and Case 1, which shows higher temperatures near windows. The 4-zonal stratum system significantly reduces temperatures compared to the baseline (23.4°C?26.8°C).

Fig. 17 shows relative humidity distribution under the 4-zonal air supply with mixing, displacement, stratum ventilation, and the baseline. In Case 1, mixing ventilation results in 40?51% humidity, with higher levels (50?51%) throughout the classroom and 47?49% in occupied zones. Case 2, with displacement ventilation, maintains 48?52% humidity. At all heights, higher relative humidity (50?52%) is observed near inlets in the north and south, decreasing toward the east (48?49%). Case 3 with stratum ventilation provides a uniform distribution (48?52%), outperforming Cases 1, 2, and the baseline (47?51%) in managing humidity and ensuring occupant comfort.

Table 9 compares PMV and PPD values at 0.1 m, 0.6 m, and 1.1 m for different ventilation cases. The 4-zonal air supply with stratum ventilation (Case 3) shows significant reductions in PMV and PPD compared to the baseline. At 0.1 m, PMV decreases by up to 48% and PPD by 53%, with similar reductions observed at 0.6 m and 1.1 m across all zones, highlighting Case 3's effectiveness. The comparative PMV and PPD plots are depicted in Fig. 18 and 19. In summary, the 4-zonal air supply with stratum ventilation design substantially reduces the PMV and PPD indices in the classroom; however, some zones still fall outside the comfort range given by ASHRAE Standard 55 [1]. Therefore, a parametric study of stratum ventilation, such as altering the heights of inlets and outlets, is recommended to achieve optimal thermal comfort.

### 3.0.2 CFD on Finding the Best Design of Stratum Ventilation with Zonal Air Supply System

At this stage, various stratum ventilation designs were investigated to find the design that provided ideal thermal comfort inside the classroom.

Fig. 20 shows air velocity distribution for stratum ventilation designs. In Case 3, velocities range from 0?0.20 m/s, with higher values (up to 0.20 m/s) in the northern area at 0.1 m and 0.6 m heights, while occupied zones have 0?0.04 m/s. At 1.1 m, velocities decrease to 0.14?0.16 m/s in the north and 0.04?0.06 m/s in student zones.

In Case 4, air velocity ranges from 0?0.15 m/s. At 0.1 m, higher velocities (0.11?0.15 m/s) are in the north but not in student zones (0?0.05 m/s). At 0.6 m, higher velocities appear in the north and south, with 0.02?0.05 m/s near students. At 1.1 m, velocities peak in the south (0.11 m/s) and rise in occupied zones to 0.05?0.09 m/s.

In Case 5, air velocity ranges from 0?0.15 m/s, with the highest values in the north and south. At 0.1 m, student zones have 0?0.03 m/s, increasing to 0.03?0.05 m/s at 0.6 m and 0.05?0.09 m/s at 1.1 m. In Case 6, velocities also range from 0?0.15 m/s and rise with height. At 0.1 m, student zones see 0?0.05 m/s, increasing to 0.03?0.05 m/s at 0.6 m and up to 0.15 m/s near inlets/outlets at 1.1 m, while middle areas range from 0.05?0.11 m/s.

In Case 7, the air velocity ranges between 0 to 0.15 m/s. At the 0.1m height, higher velocities are found in the southern part of the classroom, while lower air velocities are observed in the middle, ranging from 0 to 0.03 m/s. At the 0.6 m height, higher velocities are present in the northern and southern areas, reaching up to 0.15 m/s, with the occupied zones experiencing velocities ranging from 0.02 to 0.05 m/s. At the 1.1 m height, the highest velocities are found in the northern part of the classroom, reaching 0.15 m/s, while the middle areas, including the occupied zones, have velocities ranging between 0.05 to 0.09 m/s.

In Case 8, the air velocity ranges between 0 to 0.20 m/s. At the 0.1 m and 0.6 m heights, higher velocities are found in the southern part of the classroom, reaching up to 0.20 m/s, while in the middle of the classroom, velocities range from 0 to 0.06 m/s, with slightly higher values observed at the 0.6 m height. For the 1.1 m height, higher velocities are found in the northern part of the classroom and the middle, ranging from 0 to 0.08 m/s, with the occupied zones experiencing velocities between 0.04 to 0.06 m/s.

When comparing the stratum ventilation cases to the baseline case, the stratum cases generally offer more controlled and balanced air velocity distributions across the classroom. The baseline case tends to exhibit uneven airflow, with higher velocities concentrated near the ceiling and lower velocities near the floor, particularly in the student-occupied zones. This can result in discomfort due to drafts or inadequate air movement in key areas. Particularly, Case 8 shows improved airflow management,

with more uniform velocities across different heights. It maintains moderate velocities in the occupied zones, ensuring consistent air movement.

Fig. 21 illustrates the air temperature distribution for various stratum ventilation designs in the classroom. In Case 3, the air temperature distribution ranges between 22 °C and 25 °C. The highest temperatures, ranging from 24 °C to 25 °C, are found in the eastern part of the classroom, where the windows are located. At the 0.1 m height, cooler temperatures are observed near the student zones, ranging from 22 °C to 23 °C, while slightly warmer temperatures are found towards the edges of the classroom. At the 0.6 m height, the temperature increases slightly in the student zones, ranging from 23 °C to 24 °C. The warmest temperatures remain concentrated at the 1.1 m height, particularly near the windows.

In Case 4, the air temperature distribution ranges between 22.8 °C and 24 °C. A similar air temperature distribution is found at all heights, where higher temperatures, ranging from 23.6 °C to 24 °C, are concentrated from the middle to the south of the classroom, gradually decreasing as you move towards the north.

In Case 5, the air temperature distribution ranges between 21.8 °C and 23.5 °C. A similar air distribution pattern is found at all heights, with higher temperatures observed in the east and south, decreasing as you move toward the middle and northwest of the classroom. In the north, the temperature ranges between 22 °C and 22.8 °C, while in the middle, it ranges from 22.8 °C to 23.5 °C. In Case 6, the air temperature distribution ranges between 22 °C and 24 °C. The figures show a similar air distribution pattern at all heights, with temperatures ranging from 22.4 °C to 22.8 °C in the north and 22.8 °C to 23.6 °C in the middle. Temperatures increase as you move towards the east, reaching up to 24 °C.

In Case 5, the air temperature distribution ranges between 21.8 °C and 23.5 °C. A similar air distribution pattern is found at all heights, with higher temperatures observed in the east and south, decreasing as you move toward the middle and northwest of the classroom. In the north, the temperature ranges between 22 °C and 22.8 °C, while in the middle, it ranges from 22.8 °C to 23.5 °C.

In Case 6, the air temperature distribution ranges between 22 °C and 24 °C. The figures show a similar air distribution pattern at all heights, with temperatures ranging from 22.4 °C to 22.8 °C in the north and 22.8 °C to 23.6 °C in the middle. Temperatures increase as you move towards the east, reaching up to 24 °C.

Fig. 22 illustrates the relative humidity distribution for various stratum ventilation designs in the classroom. In Case 3, the relative humidity ranges between 48% and 50%. The relative humidity distribution follows the same pattern across all heights. The highest relative humidity, ranging from 51% to 52%, is observed in the northern part of the classroom. The occupied zones within the classroom have relative humidity levels ranging from 49% to 50%. At the 1.1 m height, relative humidity is better distributed and decreases moving towards the south

and southeast of the classroom.

In Case 4, the overall relative humidity ranges between 38% and 53%. At all heights, the highest relative humidity is observed in the northern part of the classroom, ranging between 51% and 53%, extending towards the center. The lowest relative humidity is found in the second row of the occupied zones, very close in front of the students, ranging from 38% to 42%. The middle area of the classroom ranges from 48% to 50%, with humidity increasing towards the center, reaching between 50% and 53%. The southern part of the classroom shows relative humidity levels ranging between 50% and 51%.

In Case 5, the relative humidity ranges between 47% and 51%. The contours at all heights show the same distribution pattern, with higher relative humidity observed in the northern part of the classroom, ranging from 50% to 51%. As moving to the south, the relative humidity lowers, ranging from 48% to 50% in the middle of the classroom and around 47% to 48% in the southeast. In Case 6, the relative humidity ranges between 48% and 51%, showing a smaller range than the other stratum ventilation designs. At all heights, the highest relative humidity is observed in the northern part of the classroom, ranging from 50% to 51%, and it decreases slightly as you move toward the south. The lowest relative humidity is shown in the southeast of the classroom, averaging around 48%.

Both Case 7 and Case 8 show almost the same relative humidity distribution at all heights, ranging from 48% to 52%. The highest relative humidity is observed in the northern part of the classroom, ranging from 51% to 52%. In the middle area, where the occupied zones are located, relative humidity ranges between 49% and 51%, while the southern areas range between 49% and 50%. The lowest relative humidity is observed in the southeast of the classroom, averaging around 48%.

Overall, Case 8 and Case 7 exhibit the most consistent and balanced relative humidity distribution, ranging from 48% to 52% across the classroom. Case 6 and Case 5 also perform well but show slightly less humidity in the southern areas. Case 4 displays the widest relative humidity range, from 38% to 53%, with the lowest values in the occupied zones, making it less ideal. Case 3 has a narrower range of 48% to 50% but with less uniformity than Cases 6 and 7.

Table 10 compares the PMV and PPD values at 0.1 m, 0.6 m, and 1.1 m in the classroom between the baseline case (mixing ventilation) and the 4-zonal stratum ventilation cases. The table demonstrates that utilizing a 4-zonal air supply with stratum ventilation (Inlet at 1 m outlet at 0.2 m above the floor) resulted in the most significant reduction of PMV and PPD values across all heights compared to the other cases.

**Table 5:** Properties of the human body, ASHRAE Standard-55 [1].

Properties	Value
Density ( $m^3/kg$ )	985
Temperature ( $^{\circ}C$ )	37
Metabolic rate ( $W$ )	150
Specific heat ( $J/kg.K$ )	2500
Thermal conductivity ( $kg/ms$ )	0.45
Heat generation ( $W/m^3$ )	15

**Table 6:** GCI for different mesh sizes.

	Refinement ratio ( $r$ )		Relative difference ( $\epsilon$ )		Order of accuracy ( $P$ )		Grid Convergence Indices ( $GCI$ )	
	$r_{21}$	$r_{32}$	$\epsilon_{21}$	$\epsilon_{32}$	$P_{21}$	$P_{32}$	$GCI_{21}$	$GCI_{32}$
Air temperature	1.381	1.324	-0.121	0.0024	10	12	0.32	0.016
Air velocity	1.381	1.324	-0.0082	0.0091	6.8	9	0.166	0.039

**Table 7:** Properties of the mesh.

Size	Mesh metric		
Maximum	0.0819 m	Skewness (close to 0)	0.13
Minimum	0.00001	Orthogonal quality (close to 1)	0.98
Curvature normal angle	18 $^{\circ}C$	Element quality (close to 1)	0.99
Growth rate	1.2		

**Table 8:** Examined zonal air supply cases.

	Size	Mesh metric
Case 1	4-zonal (Mixing ventilation)	$V_{inlet} = 0.5m/s$
Case 2	4-zonal (Displacement ventilation)	$V_{inlet} = 0.5m/s$
Case 3	4-zonal Stratum ventilation (inlet and Outlet at 0.2 m above the floor)	$V_{inlet} = 0.5m/s$
Case 4	4-zonal Stratum ventilation (inlets at 0.2 m and outlets at 1 m above the floor)	$V_{inlet} = 0.5m/s$
Case 5	4-zonal Stratum ventilation (inlets and Outlet at 0.5 m above the floor)	$V_{inlet} = 0.5m/s$
Case 6	4-zonal Stratum ventilation (inlets and Outlet at 1.0 m above the floor)	$V_{inlet} = 0.5m/s$
Case 7	4-zonal Stratum ventilation (inlets at 0.5 m and outlets at 0.2 m above the floor)	$V_{inlet} = 0.5m/s$
Case 8	4-zonal Stratum ventilation (inlets at 1.0 m and outlets at 0.2 m above the floor)	$V_{inlet} = 0.5m/s$

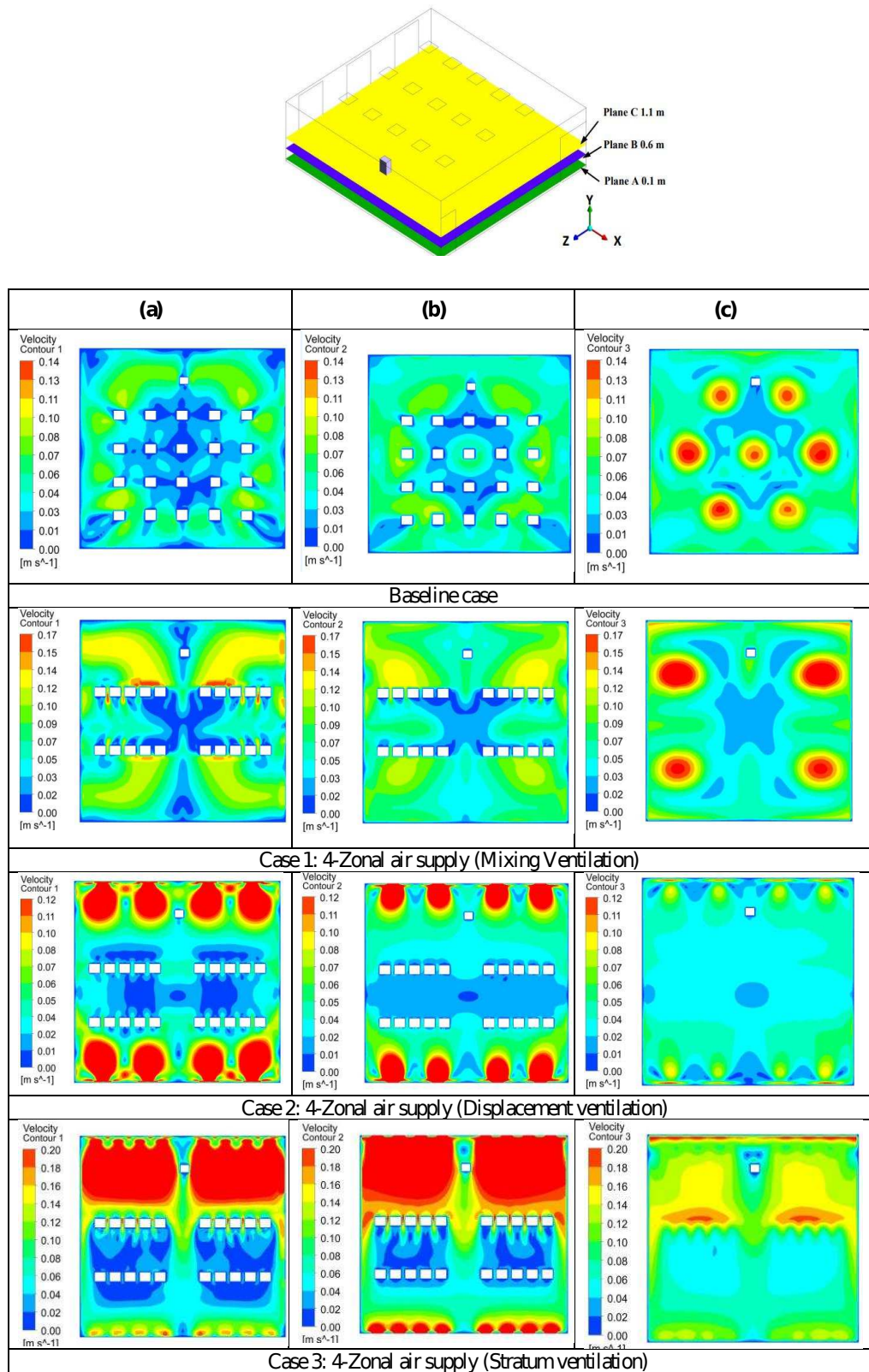


**Fig. 15:** The Air velocity distribution (a) In-plane A, 0.1 m (b) In-plane B, 0.6 m (c) In-plane C, 1.1 m of 4-zonal air supply cases (Mixing ventilation, Displacement ventilation, and Stratum ventilation) with the baseline case.

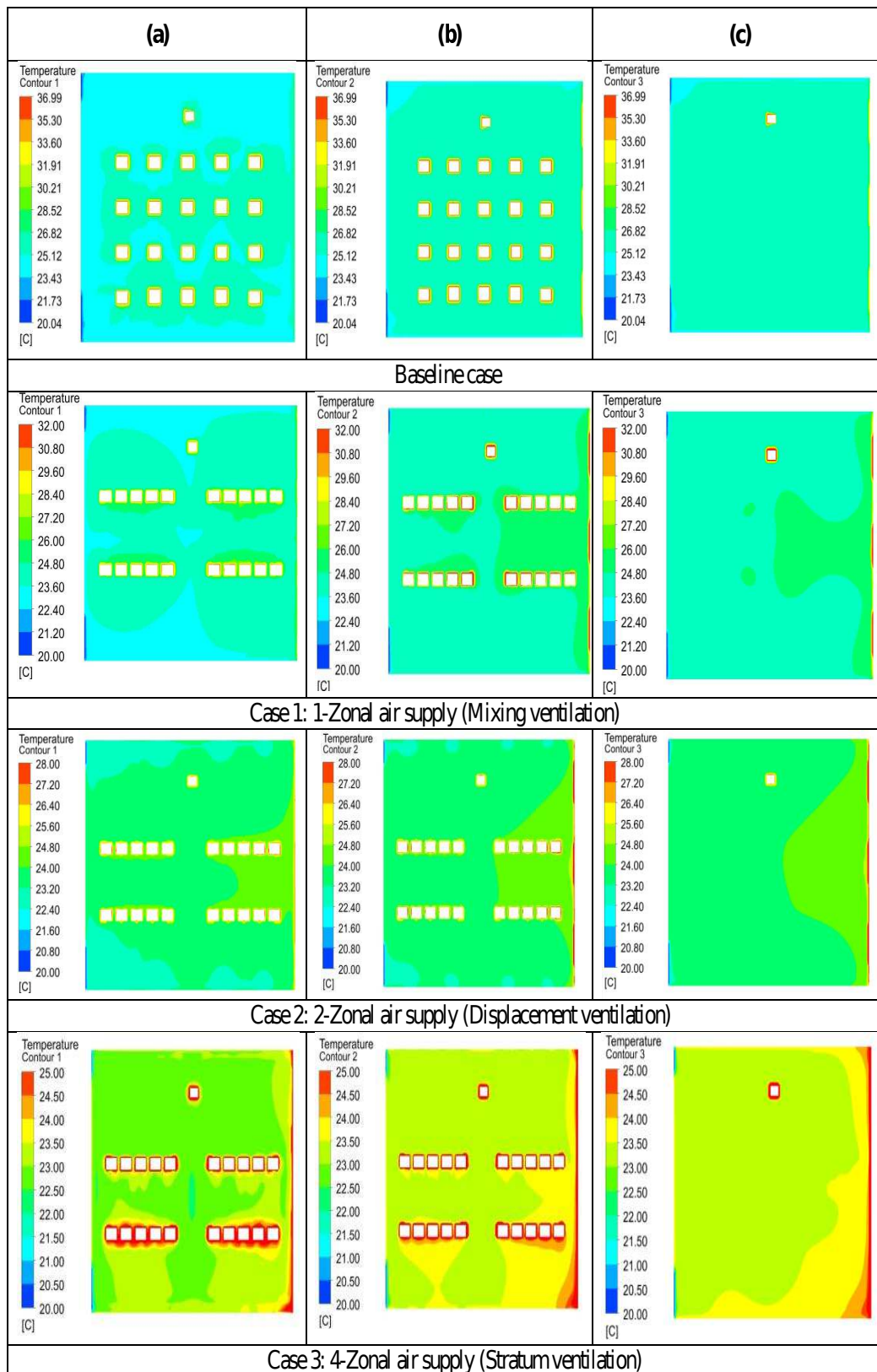


**Fig. 16:** The Air temperature distribution (a) In-plane A, 0.1 m (b) In-plane B, 0.6 m (c) In-plane C, 1.1 m of 4-zonal air supply cases (Mixing ventilation, Displacement ventilation, and Stratum ventilation) with the baseline case .

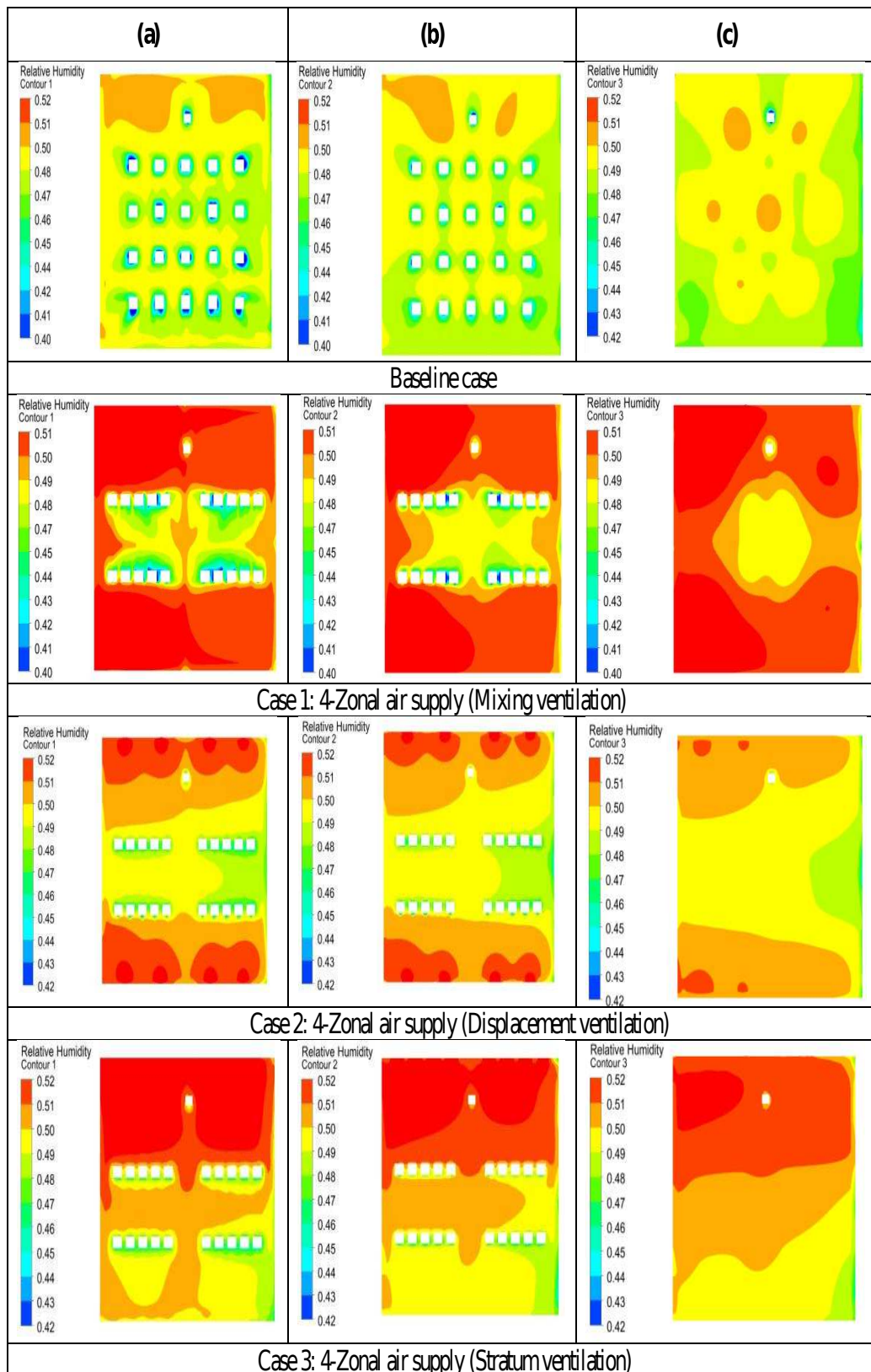


**Fig. 17:** The relative humidity distribution (a) In-plane A, 0.1 m (b) In-plane B, 0.6 m (c) In-plane C, 1.1 m of 4-zonal air supply cases (Mixing ventilation, Displacement ventilation, and Stratum ventilation) with the baseline case .

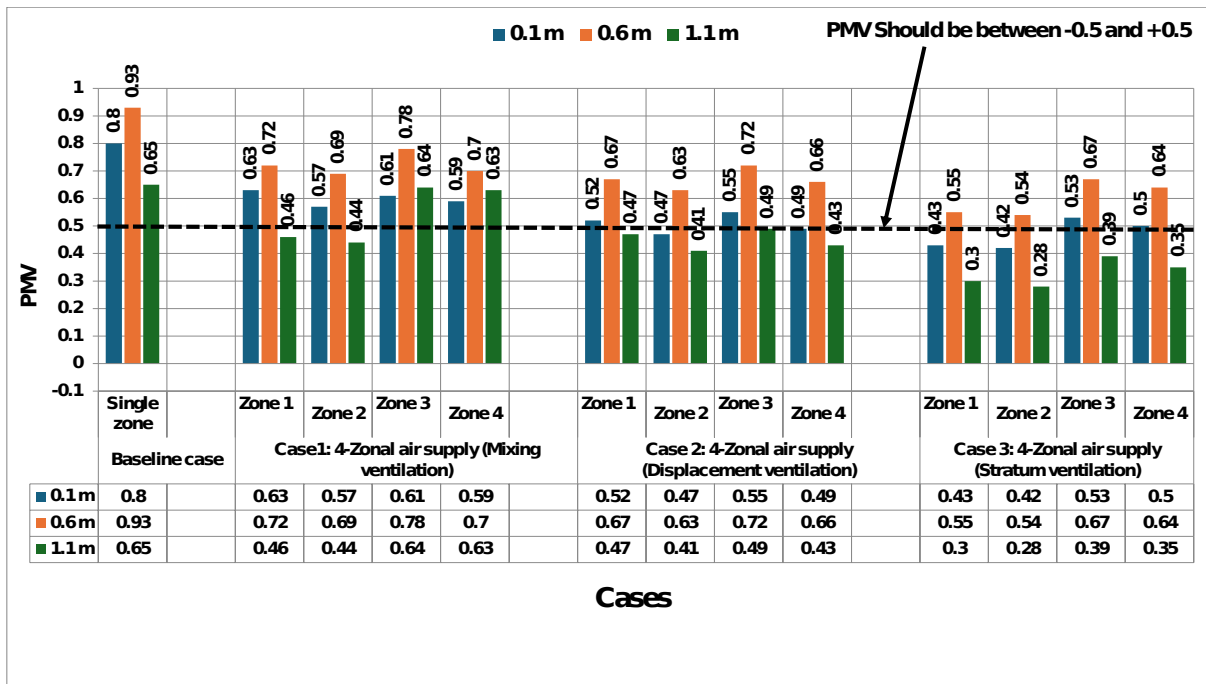


Fig. 18: Comparison of PMV values of 4-zonal air supply cases (Mixing, Displacement, and Stratum ventilation) with the baseline case at different heights.

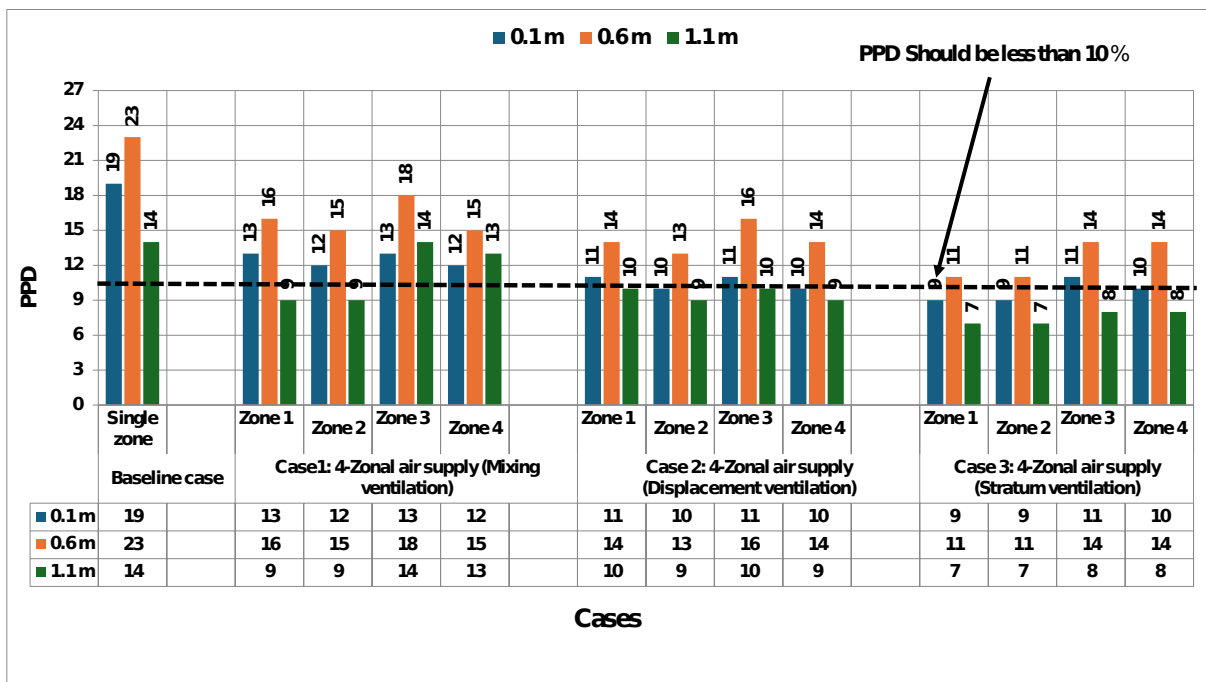
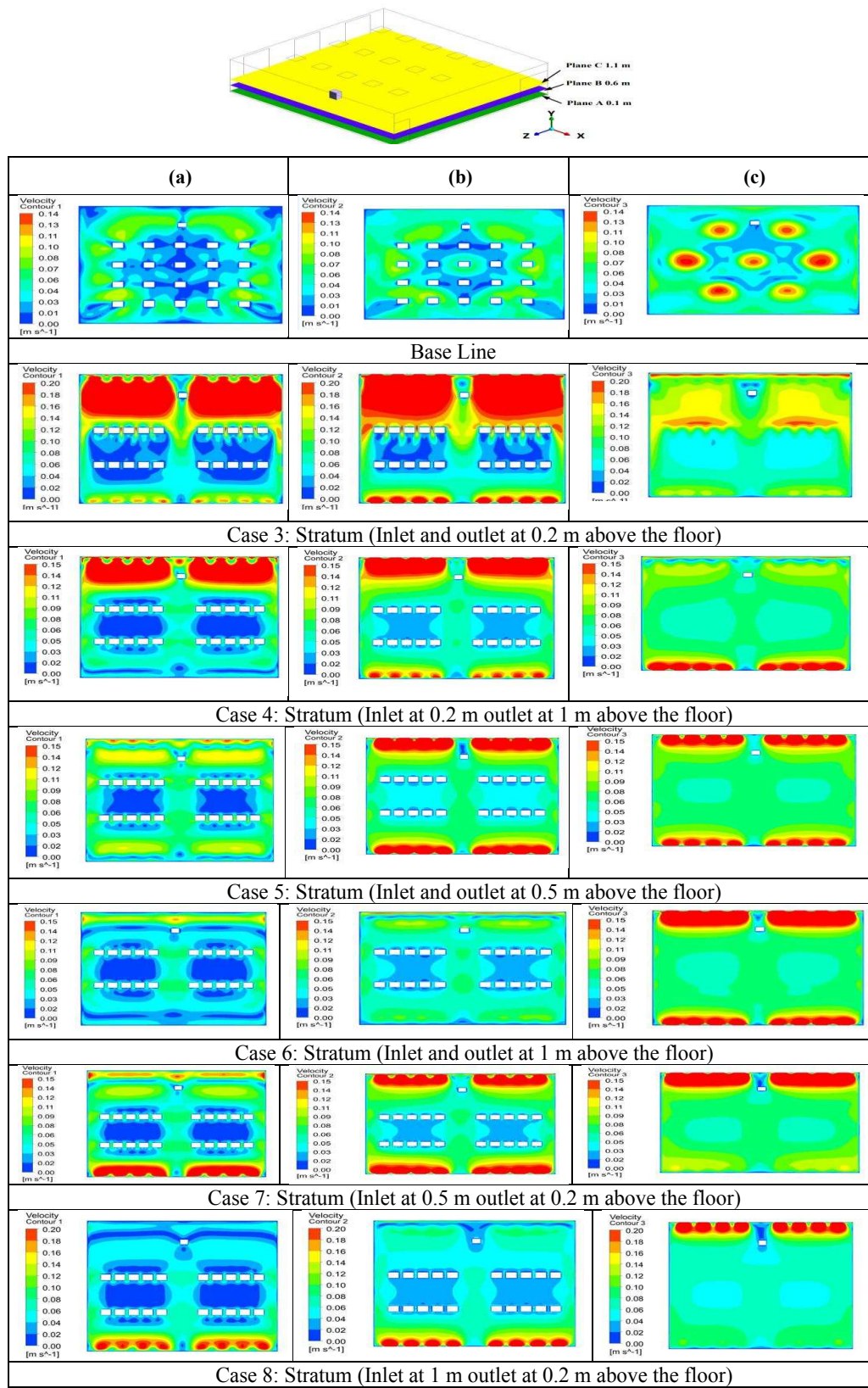
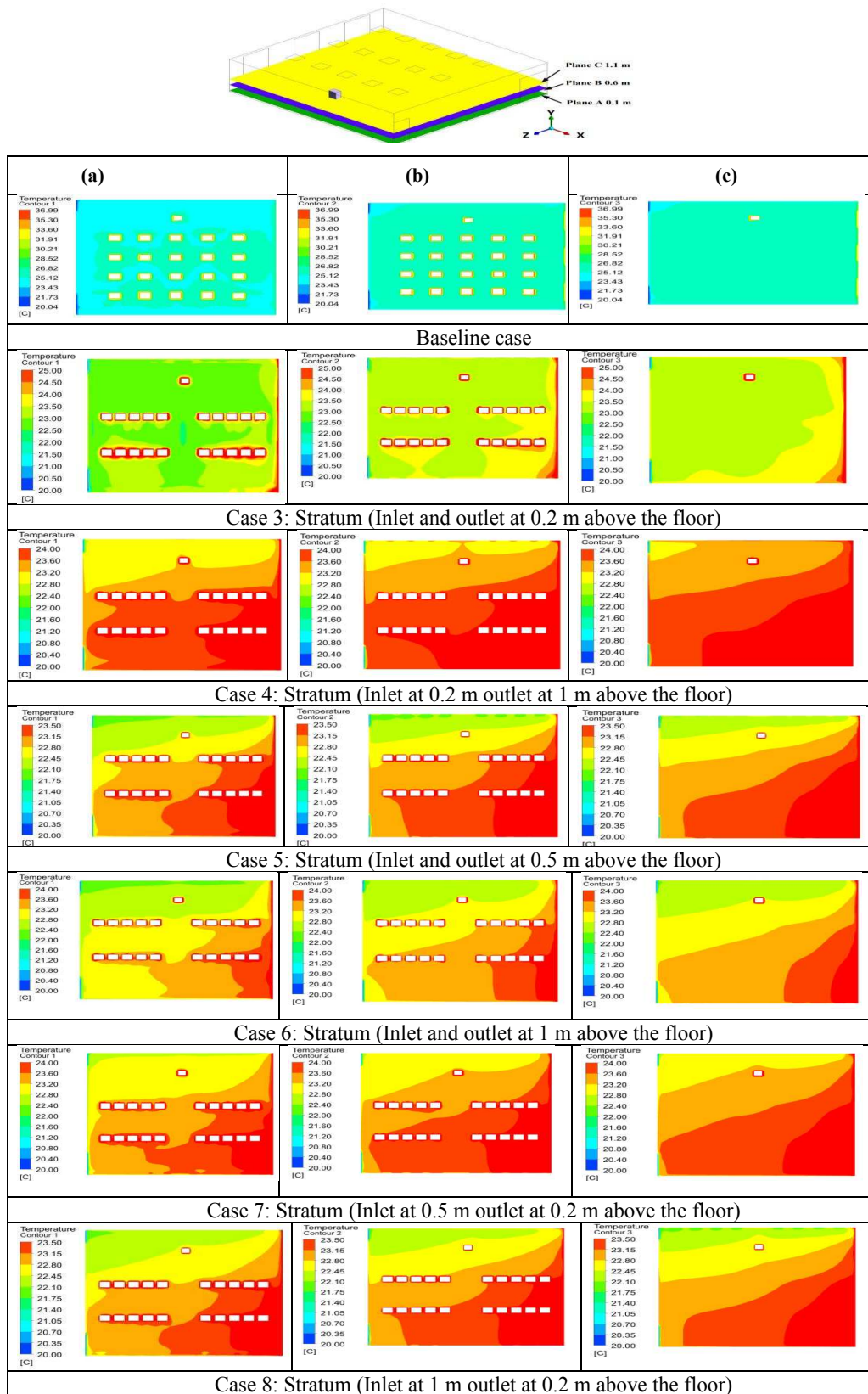


Fig. 19: Comparison of PPD values of 4-zonal air supply cases (Mixing, Displacement, and Stratum ventilation) with the baseline case at different heights.



**Fig. 20:** The air velocity distribution (a) In plane A, 0.1 m (b) In plane B, 0.6 m (c) In plane C, 1.1 m of 4-zonal air supply with different designs of stratum ventilation and the baseline case.



**Fig. 21:** The air temperature distribution (a) plane A, 0.1 m (b) plane B, 0.6 m (c) plane C, 1.1 m of 4-zonal air supply with different designs of stratum ventilation and the baseline case.

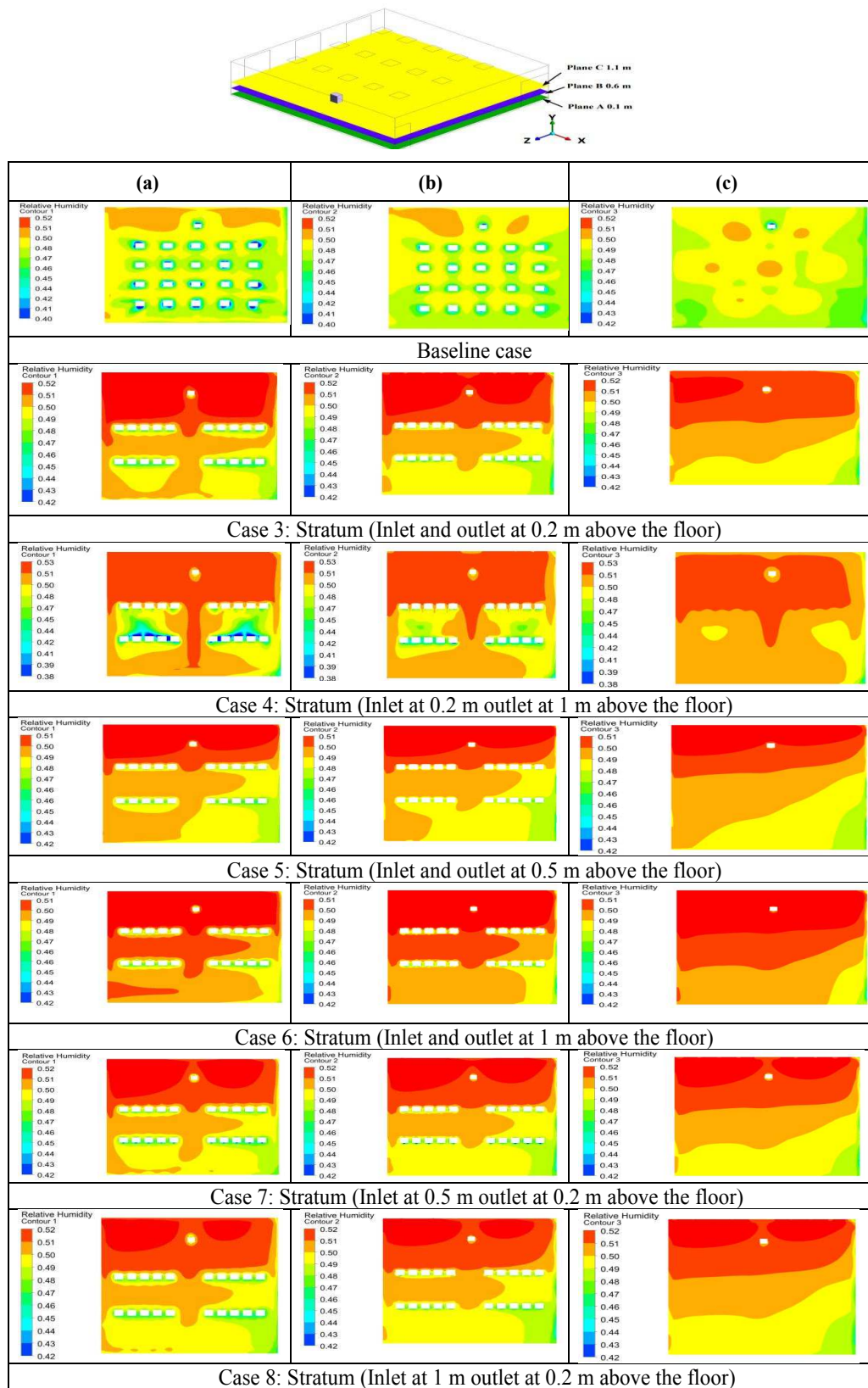


**Fig. 22:** The relative humidity distribution (a) plane A, 0.1 m (b) plane B, 0.6 m (c) plane C, 1.1 m of 4-zonal air supply with different designs of stratum ventilation and the baseline case.

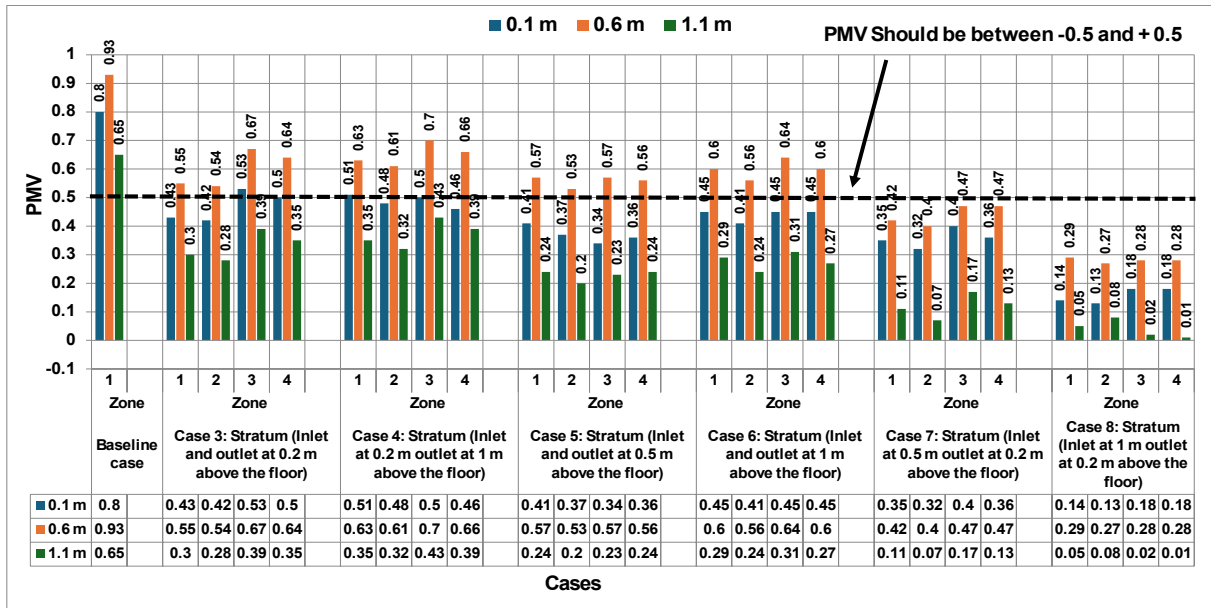


Fig. 23: Comparison of PMV values of 4-zonal air supply using various stratum ventilation designs in different heights.

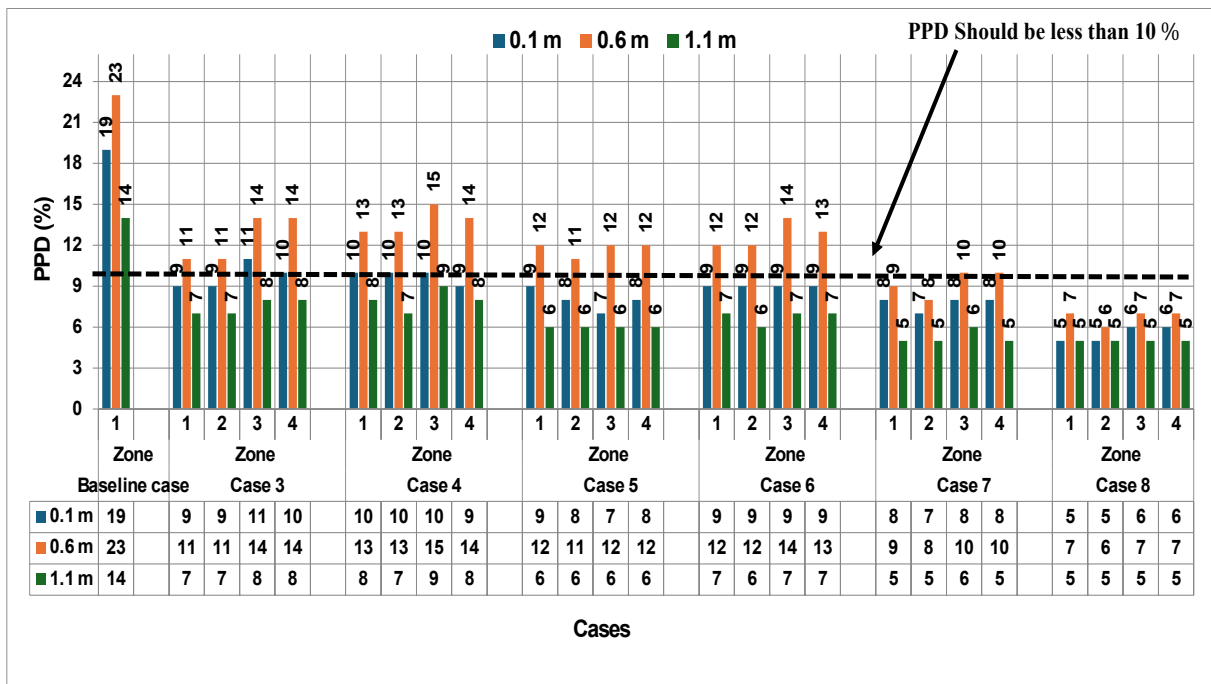
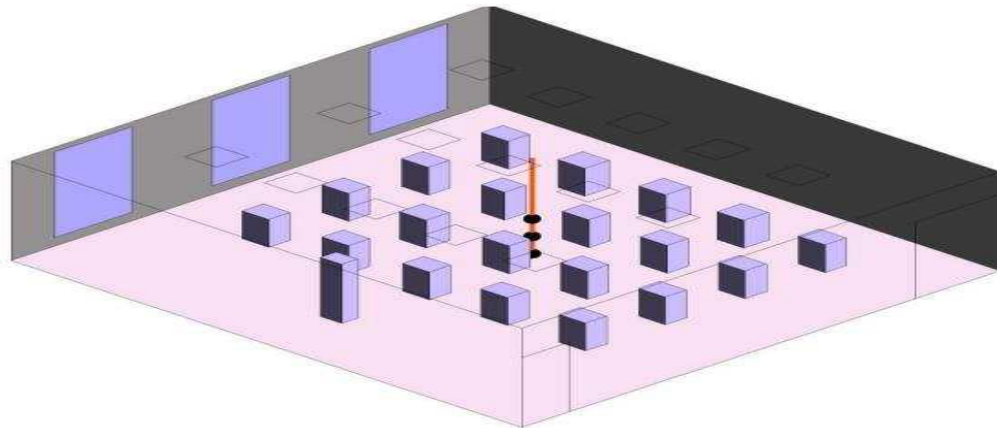


Fig. 24: Comparison of PPD values of 4-zonal air supply using various stratum ventilation designs in different heights.



**Fig. 25:** comparison of the PMV and PPD values in the classroom between the baseline case (mixing ventilation) and the 4-zonal stratum ventilation cases.

**Table 9:** Comparison of PMV and PPD values of 4-zonal air supply with the baseline case.

Case	Zone	PMV			PPD%		
		Height (m)			Height (m)		
		0.1	0.6	1.1	0.1	0.6	1.1
Baseline (See Fig. 25)	Single zone	0.80	0.93	0.65	19	23	14
Case 1 (4-Zonal air supply(mixing ventilation)) (See Fig. 14)	Zone 1	0.63	0.72	0.46	13	16	9
	Zone 2	0.57	0.69	0.44	12	15	9
	Zone 3	0.61	0.78	0.64	13	18	14
	Zone 4	0.59	0.70	0.63	12	15	13
Case 2 (4-Zonal air supply(displacement ventilation)) (See Fig. 14)	Zone 1	0.52	0.67	0.47	11	14	10
	Zone 2	0.47	0.63	0.41	10	13	9
	Zone 3	0.55	0.72	0.64	13	18	14
	Zone 4	0.49	0.66	0.43	10	14	9
Case 3 (4-Zonal air supply(stratum ventilation)) (See Fig. 14)	Zone 1	0.43	0.55	0.30	9	11	7
	Zone 2	0.42	0.54	0.28	9	11	7
	Zone 3	0.53	0.67	0.39	11	14	8
	Zone 4	0.50	0.64	0.35	10	14	8

**Table 10:** PMV and PPD values of the 4-zonal air supply with stratum ventilation cases compared to the baseline case.

Case	Zone	PMV				PPD%	
		Height (m)		Height (m)		Height (m)	
		0.1	0.6	1.1	0.1	0.6	1.1
Baseline (See Fig. 25)	Single zone	0.80	0.93	0.65	19	23	14
Case 3 (ventilation (Inlet and outlet at 0.2 m above the floor)) (See Fig. 14)	Zone 1	0.43	0.55	0.30	9	11	7
	Zone 2	0.42	0.54	0.28	9	11	7
	Zone 3	0.53	0.67	0.39	11	14	8
	Zone 4	0.50	0.64	0.35	10	14	8
Case 4 (ventilation (Inlet at 0.2 m and outlet at 1 m above the floor)) (See Fig. 14)	Zone 1	0.51	0.63	0.35	10	13	8
	Zone 2	0.48	0.61	0.32	10	13	8
	Zone 3	0.50	0.70	0.43	10	15	9
	Zone 4	0.46	0.66	0.39	9	14	8
Case 5 (ventilation (Inlet and outlet at 0.5 m above the floor)) (See Fig. 14)	Zone 1	0.41	0.57	0.24	9	12	6
	Zone 2	0.37	0.53	0.20	8	11	6
	Zone 3	0.34	0.57	0.23	7	12	6
	Zone 4	0.36	0.56	0.24	8	12	6
Case 6 (ventilation (Inlet and outlet at 1 m above the floor)) (See Fig. 14)	Zone 1	0.45	0.60	0.29	9	12	7
	Zone 2	0.41	0.56	0.24	9	12	6
	Zone 3	0.45	0.64	0.31	9	14	7
	Zone 4	0.45	0.60	0.27	9	13	7
Case 7 (ventilation (Inlet at 0.5 m and outlet at 0.2 m above the floor)) (See Fig. 14)	Zone 1	0.35	0.42	0.11	8	9	5
	Zone 2	0.32	0.40	0.07	7	8	5
	Zone 3	0.40	0.47	0.17	8	10	6
	Zone 4	0.36	0.47	0.13	8	10	5
Case 8 (ventilation (Inlet at 1 m and outlet at 0.2 m above the floor)) (See Fig. 14)	Zone 1	0.14	0.29	0.05	5	7	5
	Zone 2	0.13	0.27	0.08	5	6	5
	Zone 3	0.18	0.28	0.02	6	7	5
	Zone 4	0.18	0.28	0.01	6	7	5

Compared with the baseline case, Table 10 reveals that when using the 4-zonal air supply with stratum ventilation design (Inlet at 1 m outlet at 0.2 m above the floor) at the height of 0.1 m, the PMV values are reduced by 83%, 84%, 78%, and 78%. In contrast, the PPD values are reduced by 74%, 74%, 68%, and 68% in zones 1, 2, 3, and 4, respectively. At the height of 0.6 m, the PMV values are reduced by 69%, 71%, 70%, and 70%, while the PPD values see reductions of 70%, 74%, 70%, and 70% in zones 1, 2, 3, and 4, respectively. At the height of 1.1 m, the PMV values are reduced by 92%, 88%, 97%, and 98%, while the PPD values are reduced by 64%, 64%, 64%, and 64% in zones 1, 2, 3, and 4, respectively. The comparative plots of the PMV and PPD values are illustrated [52, 53, 54] in Fig. 23 and Fig. 24. Results indicate that according to the ASHRAE standard-55 [1], the ideal scenario resulting in optimal thermal comfort in the classroom was achieved by the 4-zonal air supply design with stratum ventilation (Inlet at 1 m outlet at 0.2 m above the floor), as PMV at all heights and zones fell between -0.5 and +0.5, and PPD was less than 10%.

## 4 Conclusions

This research investigates thermal comfort inside a classroom at the University of Business and Technology, Jeddah, Saudi Arabia, under the existing ventilation, considering the PMV and PPD indices. Field measurements were carried out in July to evaluate thermal comfort in the classroom. The results indicate that the indices are out of the ASHRAE-55 range. The effects of utilizing a zonal air supply on thermal comfort inside the classroom under mixing, displacement, and stratum ventilation using the CFD method revealed an improvement in the thermal condition, especially when using stratum ventilation. Therefore, five cases of zonal air supply systems with stratum ventilation were tested through a parametric study to discover which case would produce the highest reductions in the indices. It was discovered that using the 4-zonal air supply with stratum ventilation such that the inlets and outlets are positioned at 1 m outlet at 0.2 m, respectively, above the floor) can reduce the PMV by 78% - 84%, 69% - 71%, and 88% - 92% for the heights 0.1 m, 0.6 m and 1.1 m, respectively. Also, the PPD values have been reduced by 68%-74%, 70%-74%, and 64% for the heights 0.1 m, 0.6 m, and 1.1 m, respectively. This study successfully found an innovative design that enhanced classroom thermal comfort under Jeddah's climatic conditions.

### Acknowledgment

This project was funded by the Deanship of Scientific Research (DSR), University of Business and Technology, Jeddah-Saudi Arabia. The authors, therefore, gratefully acknowledge the DSR technical and financial support.

### Funding

This project was fully funded by the Deanship of

Scientific Research (DSR), University of Business and Technology, Jeddah-Saudi Arabia.

### Conflict of Interest

Has no conflict of Interest.

### Ethical Approval

This article does not contain any studies with animals performed by any of authors.

### Consent to Participate

Consent to participate.

### Consent to Publish

Consent to publish

### Data availability statement

All data generated or analyzed during this study are included in this published article.

### Author Contributions

All authors contributed to the study conception and design. Material preparation, data collection and analysis were performed.

### Declaration of competing interest

The authors declare that they have no known competing financial interests or personal relationships that could have appeared to influence the work reported in this paper.

## References

- [1] Standard, A.S.H.R.A.E., 2020. Thermal environmental conditions for human occupancy. ANSI/ASHRAE, 55, 5.
- [2] P. Heiselberg, S. Murakami and C.A. Roulet, Ventilation of large spaces in buildings. Final Report IEA Annex 26, (1998).
- [3] Q. Chen, Ventilation performance prediction for buildings: A method overview and recent applications. *Building and Environment* 44(4), pp.848-858 (2009).
- [4] H. Al-Khatri, M. Alwetaishi and M.B. Gadi, Exploring thermal comfort experience and adaptive opportunities of female and male high school students. *Journal of Building Engineering*, 31, p.101365 (2020).
- [5] I. Reda, R.N. AbdelMessih, M. Steit and E.M. Mina, Quantifying fenestration effect on thermal comfort in naturally ventilated classrooms. *Sustainability*, 13(13), p.7385 (2021).
- [6] H. Alzahrani, M. Arif, A. Kaushik, J. Goulding and D. Heesom, Artificial neural network analysis of teachers' performance against thermal comfort. *International Journal of Building Pathology and Adaptation*, 39(1), pp.20-32 (2021).
- [7] M. Bayoumi, Improving natural ventilation conditions on semi-outdoor and indoor levels in warm/humid climates. *Buildings*, 8(6), p.75 (2018).
- [8] S.H. Ibrahim, A. Baharun, M.M. Nawi and E. Junaidi, Analytical studies on levels of thermal comfort in typical low-income houses design. *Journal of Civil Engineering, Science and Technology*, 5(1), pp.28-33 (2014).
- [9] M.S. Al-Homoud, A.A. Abdou and T.M. Budaiwi, Assessment of monitored energy use and thermal comfort conditions in mosques in hot-humid climates. *Energy and Buildings*, 41(6), pp.607-614 (2009).
- [10] P. Rajagopalan and M.B. Luther, Thermal and ventilation performance of a naturally ventilated sports hall within an aquatic centre. *Energy and buildings*, 58, pp.111-122 (2013).

- [11] A. Hussin, E. Salleh, H.Y. Chan and S. Mat, Thermal comfort during daily prayer times in an air-conditioned mosque in Malaysia. 8th Windsor Conference, 10-13 April, (2014), Windsor UK.
- [12] M. Hajdukiewicz, M. Geron and M.M. Keane, Calibrated CFD simulation to evaluate thermal comfort in a highly glazed naturally ventilated room. *Building and Environment*, **70**, pp.73-89 (2013).
- [13] International Organization for Standardization, Ergonomics of the thermal environment: Analytical determination and interpretation of thermal comfort using calculation of the PMV and PPD indices and local thermal comfort criteria. International Organization for Standardization (2005).
- [14] J.M. Villafruela, I. Olmedo, M.R. De Adana, C. Méndez, and P.V. Nielsen, CFD analysis of the human exhalation flow using different boundary conditions and ventilation strategies. *Building and Environment*, **62**, pp.191-200 (2013).
- [15] C. Younes and C. Abi Shdid, A methodology for 3-D multiphysics CFD simulation of air leakage in building envelopes. *Energy and Buildings*, **65**, pp.146-158 (2013).
- [16] K. Setaih, N. Hamza, M. Mohammed, S. Dudek and T. Townshend, CFD modeling as a tool for assessing outdoor thermal comfort conditions in urban settings in hot arid climates. *Journal of Information Technology in Construction*, **19**, pp.248-269 (2014).
- [17] M.S.M. Ali, C.J. Doolan and V. Wheatley, Grid convergence study for a two-dimensional simulation of flow around a square cylinder at a low Reynolds number. In *Seventh International Conference on CFD in The Minerals and Process Industries* (ed. PJ Witt and MP Schwarz), pp.1-6 (2009).
- [18] J.K. Calautit, D. O'Connor, P. Sofotasiou and B.R. Hughes, CFD simulation and optimisation of a low energy ventilation and cooling system. *Computation*, **3**(2), pp.128-149 (2014).
- [19] J.F. Nicol, I.A. Raja, A. Allaudin and G.N. and Jamy, Climatic variations in comfortable temperatures: the Pakistan projects. *Energy and buildings*, **30**(3), pp.261-279 (1999).
- [20] A.M.A. Rahman, Usaha-usaha mencapai keeselesaian terma dalam di Malaysia. Pulau Pinang: Universiti Sains Malaysia, (2000).
- [21] Y.C. Tung, Y.C. Shih and S.C. Hu, Numerical study on the dispersion of airborne contaminants from an isolation room in the case of door opening. *Applied Thermal Engineering*, **29**(8-9), pp.1544-1551 (2009).
- [22] K. Akbari, Impact of Radon Ventilation on Indoor Air Quality and Building Energy Saving, (2009).
- [23] A.N.Z. Sanusi, Low Energy Ground Cooling System For Buildings In Hot And Humid Malaysia?. *Journal of Architecture, Planning and Construction Management (JAPCM)*, **1**(2), (2012).
- [24] S. Hussain, Numerical investigations of the indoor thermal environment in atria and of the buoyancy-driven ventilation in a simple atrium building. Queen's University (Canada) (2012).
- [25] H.G. Tao, H.X. Chen, J.L. Xie and J.Z. Jiang, Comparison on simulation and experiment of supply air through metro vehicle air conditioning duct. *Applied Mechanics and Materials*, **44**, pp.1724-1728 (2011).
- [26] M. Woloszyn, T. Kalamees, M.O. Abadie, M. Steeman and A.S. Kalagasidis, The effect of combining a relative-humidity-sensitive ventilation system with the moisture-buffering capacity of materials on indoor climate and energy efficiency of buildings. *Building and Environment*, **44**(3), pp.515-524 (2009).
- [27] J.W. Axley, Application of Natural Ventilation for US Commerical Buildings: Climate Suitability Design Strategies and Methods Modeling Studies (2001). <https://api.semanticscholar.org/CorpusID:133885579>
- [28] G. Ye, C. Yang, Y. Chen and Y. Li, A new approach for measuring predicted mean vote (PMV) and standard effective temperature (SET\*). *Building and environment*, **38**(1), pp.33-44 (2003).
- [29] I.R. Hegazy and E.M. Qurnfulah, Thermal comfort of urban spaces using simulation tools exploring street orientation influence of on the outdoor thermal comfort: a case study of Jeddah, Saudi Arabia. *International Journal of Low-Carbon Technologies*, **15**(4), pp.594-606 (2020).
- [30] M. Attia, Sustainability features of Jeddah traditional housing. In *Sustainable housing*. IntechOpen (2021).
- [31] M. Alwetaishi, Impact of glazing to wall ratio in various climatic regions: A case study. *Journal of King Saud University-Engineering Sciences*, **31**(1), pp.6-18 (2019).
- [32] M. Bayoumi, Method to integrate radiant cooling with hybrid ventilation to improve energy efficiency and avoid condensation in hot, humid environments. *Buildings*, **8**(5), p.69 (2018).
- [33] B.S. Alotaibi, S. Lo, E. Southwood and D. Coley, Evaluating the suitability of standard thermal comfort approaches for hospital patients in air-conditioned environments in hot climates. *Building and Environment*, **169**, p.106561 (2020).
- [34] M. Balbis-Morejón, J.M. Rey-Hernández, C. Amaris-Castilla, E. Velasco-Gómez, J.F. San José-Alonso and F.J. Rey-Martínez, Experimental study and analysis of thermal comfort in a university campus building in tropical climate. *Sustainability*, **12**(21), p.8886 (2020).
- [35] A.L. Pertiwi, L.H. Sari and A. Munir,. Evaluation of air quality and thermal comfort in classroom. In *IOP Conference Series: Earth and Environmental Science* **881**(1), p.012028 (2021).
- [36] Y. Cheng, Z. Lin and A.M. Fong, Effects of temperature and supply airflow rate on thermal comfort in a stratum-ventilated room. *Building and Environment*, **92**, pp.269-277 (2015).
- [37] Y. Liu, Y. Liu, X. Shao, Y. Liu, C.E. Huang and Y. Jian, 2022. Demand-oriented differentiated multi-zone thermal environment: Regulating air supply direction and velocity under stratum ventilation. *Building and Environment*, **219**, p.109242 (2022).
- [38] E. ASHRAE, *ASHRAE Handbook Fundamentals*. Atlanta, GA, American Society of Heating, Refrigeration and Air-Conditioning Engineers (2013).
- [39] N.S.M. Taib, S.A. Zaki, H.B. Rijal, A. Abd Razak, A. Hagishima, W. Khalid and M.S.M Ali, Associating thermal comfort and preference in Malaysian universities? air-conditioned office rooms under various set-point temperatures. *Journal of Building Engineering*, **54**, p.104575 (2022).
- [40] H.M. Kamar, N.B. Kamsah, F.A. Ghaleb and M.I. Alhamid, Enhancement of thermal comfort in a large space building. *Alexandria Engineering Journal*, **58**(1), pp.49-65 (2019).
- [41] Eshhorfu, Impact of roof insulation materials and configurations on thermal performance in houses, hot dry climate in Libya (2018).

- [42] F. Tartarini, S. Schiavon, T. Cheung and T. Hoyt, CBE Thermal Comfort Tool: Online tool for thermal comfort calculations and visualizations. *SoftwareX*, **12**, p.100563 (2020).
- [43] Y.H. Yau, Y.K. Chuah, K.H. Chuah, U.A. Rajput and H.J. Liew, The preliminary evaluation of design guidelines of stratum ventilation in a large tropical lecture hall. *International Journal of Ventilation*, **22**(1), pp.77-99 (2023).
- [44] X. Tian, Y. Cheng, J. Liu and Z. Lin, Evaluation of sidewall air supply with the stratified indoor environment in a consultation room. *Sustainable Cities and Society*, **75**, p.103328 (2021).
- [45] Z. Zhang, X. Chen, S. Mazumdar, T. Zhang and Q. Chen, Experimental and numerical investigation of airflow and contaminant transport in an airliner cabin mockup. *Building and Environment*, **44**(1), pp.85-94 (2009).
- [46] J. Franke, A. Hellsten, H. Schlünzen and B. Carissimo, May. The Best Practise Guideline for the CFD simulation of flows in the urban environment: an outcome of COST 732. In *The Fifth International Symposium on Computational Wind Engineering* **15**, pp.1-10 (2010).
- [47] Z. Gao and J.S. Zhang, Numerical analysis for evaluating the 'Exposure Reduction Effectiveness' of room air cleaners. *Building and Environment*, **45**(9), pp.1984-1992 (2010).
- [48] T. van Hooff, B. Blocken, L. Aanen and B. Bronsema, A venturi-shaped roof for wind-induced natural ventilation of buildings: wind tunnel and CFD evaluation of different design configurations. *Building and Environment*, **46**(9), pp.1797-1807 (2011).
- [49] P.J. Roache, Perspective: A Method for Uniform Reporting of Grid Refinement Studies. *ASME. J. Fluids Eng*, **116**(3): 405-413 (1994).
- [50] Eça, L., Hoekstra, M. and P. Roache, Verification of Calculations: an Overview of the 2nd Lisbon Workshop. In *18th AIAA computational fluid dynamics conference*, p.4089 (2007).
- [51] I.B. Celik, U. Ghia, P.J. Roache and C.J. Freitas, Procedure for estimation and reporting of uncertainty due to discretization in CFD applications. *Journal of Fluids Engineering-Transactions of the ASME*, **130**(7), pp. 1-9 (2008).
- [52] Z. Jastaneyah, H.M. Kamar and H. AL Garalleh, A Review Paper on Thermal Comfort and Ventilation Systems in Educational Buildings: Nano-Mechanical and Mathematical Aspects. *Journal of Nanofluids*, **12**(1), pp.1-17 (2023).
- [53] Z. Jastaneyah, H.M. Kamar, A. Alansari and H. AL Garalleh, A Comparative Analysis of Standard and Nano-Structured Glass for Enhancing Heat Transfer and Reducing Energy Consumption Using Metal and Oxide Nanoparticles: A Review. *Sustainability*, **15**(12), p.9221 (2023).
- [54] Jastaneyah, Z., Kamar, H.M., Hashmi, A., Ghaleb, F.A. and Al Garalleh, H., 2024. The influence of zonal air supply on thermal comfort in a classroom located in a hot and humid environment: a case study from Jeddah? Saudi Arabia. *Discover Sustainability*, **5**(1), pp.1-33.



**Zuhair Jastaneyah** is a lecturer at the college of engineering, University of Business and Technology since 2016. I have a bachelor degree in mathematics (2011) and master degree in applied mathematics (2015). My areas of interest include. Heat transfer, Thermal comfort, Ventilation systems, Computational fluid dynamics, and Mathematical modeling



**Haslinda Mohamed Kamar** is a lecturer at the School of Mechanical Engineering, Faculty of Engineering, Universiti Teknologi Malaysia (UTM) in Johor Bahru, Johor. I have been a faculty member since 1993. I teach Heat Transfer and Thermodynamics courses. My areas of interest include automotive air-conditioning, thermal comfort, indoor air quality (IAQ), natural ventilation as a passive cooling strategy in buildings, and Computational Fluid Dynamics (CFD) modeling and simulations.



**Ahmad Hashmi** is a seasoned professional with 16+ years of experience in architecture, real estate, and higher education. He earned his PhD in Construction Project Management from the University of Salford, UK, and holds an architecture degree from King Abdulaziz University. Dr. Hashmi excels in leading complex projects and developing impactful academic programs. His research focuses on construction management, sustainable design, and innovative construction methods to enhance the built environment. He actively contributes to both academia and industry, fostering collaboration and driving innovation in architectural practices.



**Fawaz Ahmed Ghaleb Noman** holds a Ph.D. in Mechanical Engineering from the University of Technology Malaysia (2017), where he conducted research on the effect of ventilation fans on thermal comfort in medium-sized mosques. He also earned his M.Sc. (2007)

and B.Sc. (1999) in Mechanical Engineering from the University of Aden, Yemen, focusing on cutting force components in metal machining and heat balance in diesel power plants, respectively. His research interests span modeling and simulation, computational fluid dynamics (CFD), engineering methodologies, and thermal comfort in buildings. Dr. Fawaz is passionate about enhancing thermal comfort and air quality through innovative engineering solutions.



**Hakim AL Garalleh** was born on 31th of May 1980, had achieved the Bachelor degree in 2003. I then got job to work as a teacher in the Ministry of Education since 2003 till 2007. In 2007, I got an acceptance to do the Master degree in Applied Mathematics then it was done

2009. The step after, I started my Ph.D. which focuses on studying modelling in Nanobiotechnology applications. Interestingly, we investigate the usefulness of carbon nanostructures for drug delivery and diseases. I have achieved 20 distinct publications in very high class journals and still working on new journal publications in the field of nanotechnology. I have been working as a lecturer and researcher since 2014 at the college of Engineering, University of Business and Technology, Saudi Arabia.